UNCLASSIFIED

MARTIN MARIETTA ENERGY SYSTEMS LIBRARIES
3 4456 0361173 1

CENTRAL RESEARCH LIBRARY
DOCUMENT COLLECTION

ORNL-2344 cy. 4
Metallurgy and Ceramics

PHASE DIAGRAM STUDIES OF ZIRCONIUM WITH SILVER, INDIUM, AND ANTIMONY

J. O. Betterton, Jr.
J. H. Frye, Jr.
D. S. Easton

CENTRAL RESEARCH LIBRARY
DOCUMENT COLLECTION

LIBRARY LOAN COPY

DO NOT TRANSFER TO ANOTHER PERSON

If you wish someone else to see this document, send in name with document and the library will arrange a loan.

OAK RIDGE NATIONAL LABORATORY
OPERATED BY
UNION CARBIDE NUCLEAR COMPANY
A Division of Union Carbide and Carbon Corporation
UCC
POST OFFICE BOX X · OAK RIDGE, TENNESSEE

UNCLASSIFIED

LEGAL NOTICE

This report was prepared as an account of Government sponsored work. Neither the United States, nor the Commission, nor any person acting on behalf of the Commission:

A. Makes any warranty or representation, express or implied, with respect to the accuracy, completeness, or usefulness of the information contained in this report, or that the use of any information, apparatus, method, or process disclosed in this report may not infringe privately owned rights; or

B. Assumes any liabilities with respect to the use of, or for damages resulting from the use of any information, apparatus, method, or process disclosed in this report.

As used in the above, "person acting on behalf of the Commission" includes any employee or contractor of the Commission to the extent that such employee or contractor prepares, handles or distributes, or provides access to, any information pursuant to his employment or contract with the Commission.

UNCLASSIFIED

ORNL-2344

Contract No. W-7405-eng-26

METALLURGY DIVISION

PHASE DIAGRAM STUDIES OF ZIRCONIUM WITH SILVER, INDIUM, AND ANTIMONY

J. O. Betterton, Jr.
J. H. Frye, Jr.
D. S. Easton

DATE ISSUED

AUG 12 1957

OAK RIDGE NATIONAL LABORATORY
Operated by
UNION CARBIDE NUCLEAR COMPANY
A Division of Union Carbide and Carbon Corporation
Post Office Box X
Oak Ridge, Tennessee

MARTIN MARIETTA ENERGY SYSTEMS LIBRARIES

3 4456 0361173 1

UNCLASSIFIED

INTERNAL DISTRIBUTION

1. C. E. Center
2. Biology Library
3. Health Physics Library
4-5. Central Research Library
6. Reactor Experimental Engineering Library
7-26. Laboratory Records Department
27. Laboratory Records, ORNL R.C.
28. Metallurgy Library
29. A. M. Weinberg
30. L. B. Emlet (K-25)
31. J. P. Murray (Y-12)
32. J. A. Swartout
33. E. H. Taylor
34. E. D. Shipley
35. M. L. Nelson
36. W. H. Jordan
37. C. P. Keim
38. R. S. Livingston
39. R. R. Dickison
40. S. C. Lind
41. F. L. Culler
42. A. H. Snell
43. A. Hollaender
44. M. T. Kelley
45. K. Z. Morgan
46. J. A. Lane
47. A. S. Householder
48. C. S. Harrill
49. C. E. Winters
50. D. S. Billington
51. D. W. Cardwell
52. D. Phillips
53. A. J. Miller
54. R. A. Charpie
55. M. J. Skinner
56. G. E. Boyd
57. C. O. Smith
58. W. W. Parkinson
59. J. H. Frye, Jr.
60. W. D. Manly
61. J. E. Cunningham
62. G. M. Adamson
63. R. J. Beaver
64. J. O. Betterton, Jr.
65. E. S. Bomar, Jr.
66. J. H. Coobs
67. R. E. Clausing
68. J. H. DeVan
69. L. M. Doney
70. D. A. Douglas, Jr.
71. D. S. Easton
72. E. Franco-Ferreria
73. R. J. Gray
74. J. P. Hammond
75. T. Hikido
76. R. L. Heestand
77-111. M. R. Hill
112. E. E. Hoffman
113. H. Inouye
114. L. K. Jetter
115. C. J. McHargue
116. R. B. Oliver
117. P. Patriarca
118. M. L. Picklesimer
119. T. K. Roche
120. G. P. Smith, Jr.
121. A. Taboada
122. R. C. Waugh
123. H. L. Yakel, Jr.
124. E. Creutz (consultant)
125. N. J. Grant (consultant)
126. H. Leidheiser, Jr. (consultant)
127. T. S. Shevlin (consultant)
128. C. S. Smith (consultant)
129. E. E. Stansbury (consultant)
130. ORNL - Y-12 Technical Library, Document Reference Section

EXTERNAL DISTRIBUTION

131. C. H. Shaw, Dept. of Physics, Ohio State University
132. E. L. Jossem, Dept. of Physics, Ohio State University
133. E. I. Salkovitz, Naval Research Laboratory, Washington
134. G. W. Lehman, Atomic International, Canoga Park, California
135. R. F. Bacher, California Institute of Technology
136. Division of Research and Development, AEC, ORO
137-571. Given distribution as shown in TID-4500 (13th ed.) under Metallurgy and Ceramics category

PHASE DIAGRAM STUDIES OF ZIRCONIUM WITH SILVER, INDIUM, AND ANTIMONY

by

J. O. Betterton, Jr., J. H. Frye, Jr. and
D. S. Easton

SUMMARY

The zirconium-rich portions of the Ag-Zr, In-Zr, and Sb-Zr phase diagrams have been determined. The variation of the phase boundaries arising from the allotropic transition in zirconium and titanium, in these systems as well as others in the literature, can be reduced to an approximate common behavior in terms of electron concentration if a metallic valency of two is used for zirconium and titanium, and if allowance is made for energy effects due to unequal sizes of atoms. Thermodynamic relations are given for these phase boundaries which with certain approximations permit the boundaries to be used to deduce relative changes of energy in the two phases with alloy composition.

INTRODUCTION

Zirconium is an element of Group IVA in the Periodic Table, with two "s" and two "d" valency electrons in the free atom, and near the beginning of the transition elements of the second Long Period. The metallic valency of transition metals is a matter of some uncertainty and this paper is part of a program which was designed to investigate the metallic valency of zirconium by determination of zirconium phase diagrams with additions of solutes: silver, cadmium, indium, tin, and antimony. The valencies of these solutes are generally regarded as 1, 2, 3, 4, and 5 and this viewpoint will be adopted in the following discussion. The position of Group IVA elements in the Periodic Table is such that with changes in the number of valency electrons in the atom, rapid changes in the melting points, interatomic spacings, compressibilities, and sublimation energies occur in the pure elements. Thus the change in the number of these electrons might be expected to have significant effects upon the phase diagrams as has been found to be the case[1] for certain alloys of copper, silver, and gold.

In view of the above, an examination of the zirconium-rich parts of the binary phase diagrams with the solutes silver, indium, and antimony has been made. These results will be described, and then compared with other zirconium and titanium phase diagrams in the literature. Finally, a discussion of the factors which affect the alpha-beta phase boundaries, arising from the allotropic transition in zirconium and titanium will be given.

EXPERIMENTAL PROCEDURE

The experimental method adopted for most of the present work was annealing and quenching in quartz capsules. Thus the investigations of the zirconium-rich portions of the Ag-Zr, In-Zr, and Sb-Zr phase diagrams were limited to temperatures less than 1300°C. In the system Ag-Zr the alloys were also investigated by thermal analysis in quartz capsules in the range 800-1000°C. The alloys were prepared by arc casting on a water cooled, copper hearth with a tungsten electrode in a pure argon atmosphere. The materials used were Grade 1 iodide zirconium from six different batches*, the analyses of which are given in Table I, silver of 99.98 per cent purity, indium of 99.99 per cent purity, and antimony of 99.95 per cent purity. Uniform solute composition was attained by multiple melting on alternate sides of the same ingot. Progressive improvements in the vacuum conditions inside the apparatus during the course of the experiments reduced the Vickers hardness change of the pure zirconium getter ingot from 3 VPN per unit melting, observed at the beginning of the program, to less than 0.5 VPN per unit melting at the end of the experiments. The casting technique finally adopted did not add a significant quantity of impurities since on three different occasions Batch No. 6 zirconium was arc cast and thereafter, isothermally annealed in the vicinity of the α/β transition. The same interval, 857-873°C, was obtained as for the original crystal bar.

The alloy ingots were annealed in silica capsules in electrically heated tube furnaces. The best method found to prevent the reaction of the zirconium with the silica was a foil wrapping of molybdenum or tantalum. With this method, test samples of iodide-zirconium of hardness 68 VPN were annealed for three days at 1200°C, quenched, and then alpha annealed. The resulting zirconium hardnesses were 67 VPN and 63 VPN with the molybdenum and tantalum foils, respectively. In most of the experiments the protection of these foils was supplemented by an additional layer of zirconium foil inside the molybdenum or tantalum foil. The alloys were in each case cold worked depending upon their ductility, outgassed at pressures in the range 10^{-5} to 10^{-7} mm Hg at a temperature which corresponded

---

*Material received from single runs of the iodide process is identified in chrononlogical order by Batches No. 1, 2, 3...Grade 1 indicates zirconium which has passed a corrosion test in steam at 316°C.

TABLE I

ANALYSES OF IODIDE ZIRCONIUM USED IN THE PHASE DIAGRAM STUDIES

Element \ Batch No. Zirconium	Spectroscopic ppm						Neutron Activation ppm					
	1	2	3	4	5	6	1	2	3	4	5	6
Ca	5	3	8	18	12	3	--	--	--	--	--	--
Cr	22	40	10	18	4	2	--	--	--	8	22	4
Cu	56	8	19	17	9	4	22	--	15	2	3	0.8
Fe	525	200	318	188	55	15	260	--	352	70	78	24
Hf	100	<700	104	190	1200	115	--	--	--	--	573	132
Mo	7	< 10	3	10	--	<10	--	--	3	0.3	6	2
Ni	40	120	69	36	12	12	63	--	90	17	13	11
Si	20	16	10	36	4	15	7	--	8	10	7	7
W	<500	--	--	<500	--	--	≤ 0.5		≤ 1	≤ 1	20	0.2

Element \ Batch No. Zirconium	Vacuum Fusion and Combustion					
	1	2	3	4	5	6
C	295	--	204	153	100	79
O	--	--	8-54	4-86	--	13-222
N	--	--	3-16	5-60	--	1-50
H	32	30	16	50	43	40
Vickers Hardness	77	83	68	60	73	58

Eighteen other elements investigated were either less than 10 ppm or in the cases phosphorous and zinc < 100 ppm. Analyses for oxygen and nitrogen depended so much upon the method used that the range of values only is indicated. The above analyses were determined at Oak Ridge National Laboratory by Mr. G. W. Leddicotte, Mr. W. A. Burns, and Mr. J. H. Edgerton.

to the final annealing temperature, cooled to room temperature, where the capsules were filled with pure argon and sealed off. The alloys were then isothermally annealed for periods of time which varied with temperature according to Table II. Whenever possible, the first anneal in the range 1000-1200°C was within a homogeneous region followed by the final anneals at the other temperatures of the phase diagram.

The temperature measurements were made with Pt/Pt + 10 per cent Rh thermocouple calibrated against the melting points of Sn, Zn, Al, Ag, Au, and Pd. The calibrations were repeated periodically so that the error due to the drift in the calibration of the thermocouple could be estimated by interpolation. For measurements in the tube furnace two other errors were considered, first the variation in temperature due to errors in the controlling instruments which was determined by frequent use of the calibrated couple, and second, the temperature gradients near the specimen, which were determined by movements of the measuring thermocouple at the start and end of each anneal. For the longer anneals the sum of the temperature errors was generally well within ± 2°C. For short time anneals and during thermal analysis the temperature error is considered to be within ± 0.5°C.

The alloys were quenched after annealing by breaking the capsule in a mixture of ice and brine by use of a foot-operated hammer. Typical times required for this operation were between two and six seconds.

The thermal analyses of the Ag-Zr alloys were made in argon-filled quartz capsules by the method of Hume-Rothery and Raynor[2]. The alloys were cast into 30- to 40-g ingots, degassed, and homogenized for 5 days at 1000°C. To investigate the extent of the segregation of silver, samples for chemical analyses were removed from three different locations on the annealed ingot. The alloys were sealed into thermal-analysis capsules with re-entrant thermocouple sheaths. Each specimen was heated for at least 15 hr in the beta phase region, cooled at 1-2°C/min. into the $(\alpha + \gamma)$ region, held 15 hr in this region and heated at 1-2°C/min. into the beta region, and then after several hours in the beta region, slowly cooled to room temperature.

TABLE II

TYPICAL ANNEALING TIMES IN PHASE DIAGRAM INVESTIGATIONS

Number of Days	Temperature °C
0.1 - 3	1200
5 - 10	1100
8 - 12	1000
15 - 25	850
20 - 30	820
30 - 45	700 - 800
45 - 60	600

The compositions of the alloys from the quenching experiments were determined by chemical analysis of the two major components or in certain more recent specimens by analysis of the solute alone. The actual microscopical samples were analyzed in this case, and prior to the analyses both sides of these specimens were investigated to insure that the specimen was not segregated. Solute depleted surface material was in every case removed by filing. The sum of the solute and solvent analyses was always well within the range 99.9 - 100.1 per cent and in general the analyses reported for different parts of the small castings prepared for microscopical work agreed with 0.3 per cent solute.*

In the course of the present experiments minor impurities in the range 0-500 ppm were found to have significant effects on certain portions of the phase diagrams, and progressive changes in the zirconium starting material and in the experimental procedure were employed to avoid some of these effects. Each diagram is thus presented in a preliminary and final version. The difference between these versions is as follows: The preliminary alloys in each system were made with iodide zirconium whose analyses are given in Table I under the designations Batches No. 1, 2, and 3. These alloys were cast under such conditions that the Vickers Hardness of pure zirconium in the alpha form was in the range 80-100 VPN when extrapolated from a curve of alloy hardness against alloy composition. These alloys contained 10-40 ppm hydrogen. The final alloys in each system were prepared from zirconium whose analyses are given in Table I under the designations Batches No. 4, 5, and 6. These alloys were cast under such conditions that the extrapolated alpha zirconium hardness was in the range 50-65 VPN. These alloys, annealed with more prolonged degassing under vacuum at elevated temperatures contained 2-10 ppm hydrogen.

A number of the alloys which were used in the various phase diagrams were analyzed by neutron activation for Cu, Fe, Mo, Ni, Si and W and for hydrogen by vacuum fusion analyses. The results are given in Table III. It will be seen

---

*The authors wish to thank Dr. J. C. Chaston and Mr. F. M. Lever of Johnson Matthey and Company, Ltd., for these analyses.

TABLE III

MINOR IMPURITY ANALYSES OF ALLOYS

Silver-Zirconium System	Neutron Activation ppm						Vacuum Fusion Analyses ppm
	Cu	Fe	Mo	Ni	Si	W	H
Preliminary Alloys	22	233	10	11	31	--	37
	38	430	17	--	--	--	15
	30	280	<0.5	≤1.5	10	42	29
			<1	≤3.0			10
Final Alloys	<1	55	14	<10	63		
	9.6	54	34	≤1.5	17	1.3	
	5.8	88	≤0.5	≤1.5	38	2.2	
	2.3	86	<0.02	--	2.2	15	
	≤3	34	≤1	--	--	≤2	
	≤3	24	≤1	11	--	≤2	2.5
	≤3	31	≤1	20	--	≤2	6.0
Indium-Zirconium System							
Preliminary Alloy	144	480	1.3	--	--	--	12
Final Alloys	18	--	6.1	49	34	--	3.8
	10	83	6.7	45	67	--	3.6
	<1	--	--	57	42	4	
	16	50	--	21	10	10	
Antimony-Zirconium System							
Final Alloys	5.6	28	<0.1	8.2	12	9	9
	7.3	30	--	1.0	15	12.5	10

that aside from the hardness* and hydrogen differences indicated in the preceding paragraph the impurity which changed the most between the preliminary and final sets of alloys was iron.

---

*The elements which are commonly associated with pronounced variations in the hardness of zirconium are oxygen, and nitrogen, both of which are known to increase the hardness value rapidly. Carbon is thought to be similar in this respect. Since the analysis for these elements involve considerable uncertainty, hardness variations are discussed as an indication of their difference in the preliminary and final alloys.

THE SILVER-ZIRCONIUM SYSTEM

Literature

The first determination of the constitution of the Ag-Zr system was by Raub and Engel[3] who found a eutectic reaction at 97 at. per cent Ag and 955°C between almost pure silver and an intermediate phase Ag-Zr. The liquidus boundary was determined from 50-100 per cent Ag by thermal analysis under conditions which contaminated the alloys. The beta phase of zirconium was later reported by Anderson, Hayes, Roberson and Kroll[4] to dissolve up to 7 at. per cent Ag. After the start of the present investigation Kemper[5] determined, with magnesium-reduced zirconium, the phase diagram which is shown in Fig. 1 (ORNL-LR-DWG 16110). Later Karlsson[6] confirmed the existence of the intermediate phase AgZr and contended that the other intermediate phase present in this system was $AgZr_3$ on the basis of an x-ray investigation of the intermediate phases in this system. Several points of difference between these two investigators and the present experiments will be treated in the discussion below.

Preliminary Investigations of the Phase Boundaries of the Alpha and Beta Phases by the Annealing Method

The results of the preliminary investigation of the phase boundaries of the alpha and beta phases by the annealing method are shown in Fig. 2 (ORNL-LR-DWG 15394). It was found that the beta phase decomposes by a eutectoid reaction

$$\beta\ (3.7 \text{ at } \%\ \text{Ag}) \rightleftarrows \alpha\ (0.1 \text{ at } \%\ \text{Ag}) + \gamma$$

at 823°C where γ is the first intermediate phase from the zirconium-rich side of this system, Zr_2Ag.

The solid solubility of silver is clearly more extensive in the beta phase of zirconium than in the alpha phase and the α/β phase boundaries* are depressed by the addition of silver. The alpha phase solid solubility is restricted to ≤ 0.1 at. per cent Ag over the whole temperature range from 600°C to 835°C. The presence

---

*The crystal structures of the alpha and beta phases are close-packed hexagonal and body centered cubic, respectively. In the present discussion the $\alpha/(\alpha + \beta)$ and $\beta/(\alpha + \beta)$ phase boundaries are called simply the α/β boundaries.

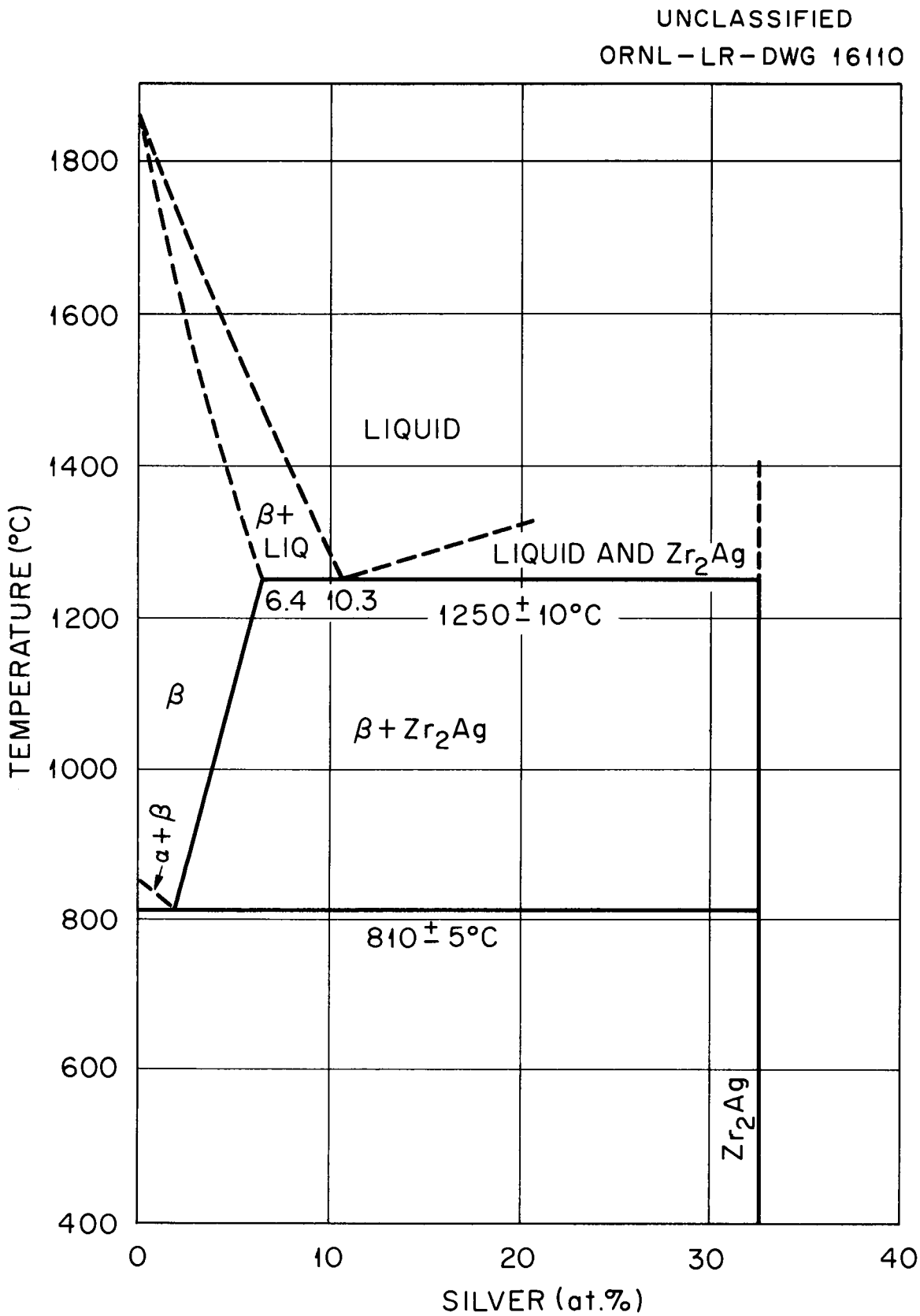

Fig.1. Silver-Zirconium Equilibrium Diagram According to Kemper.

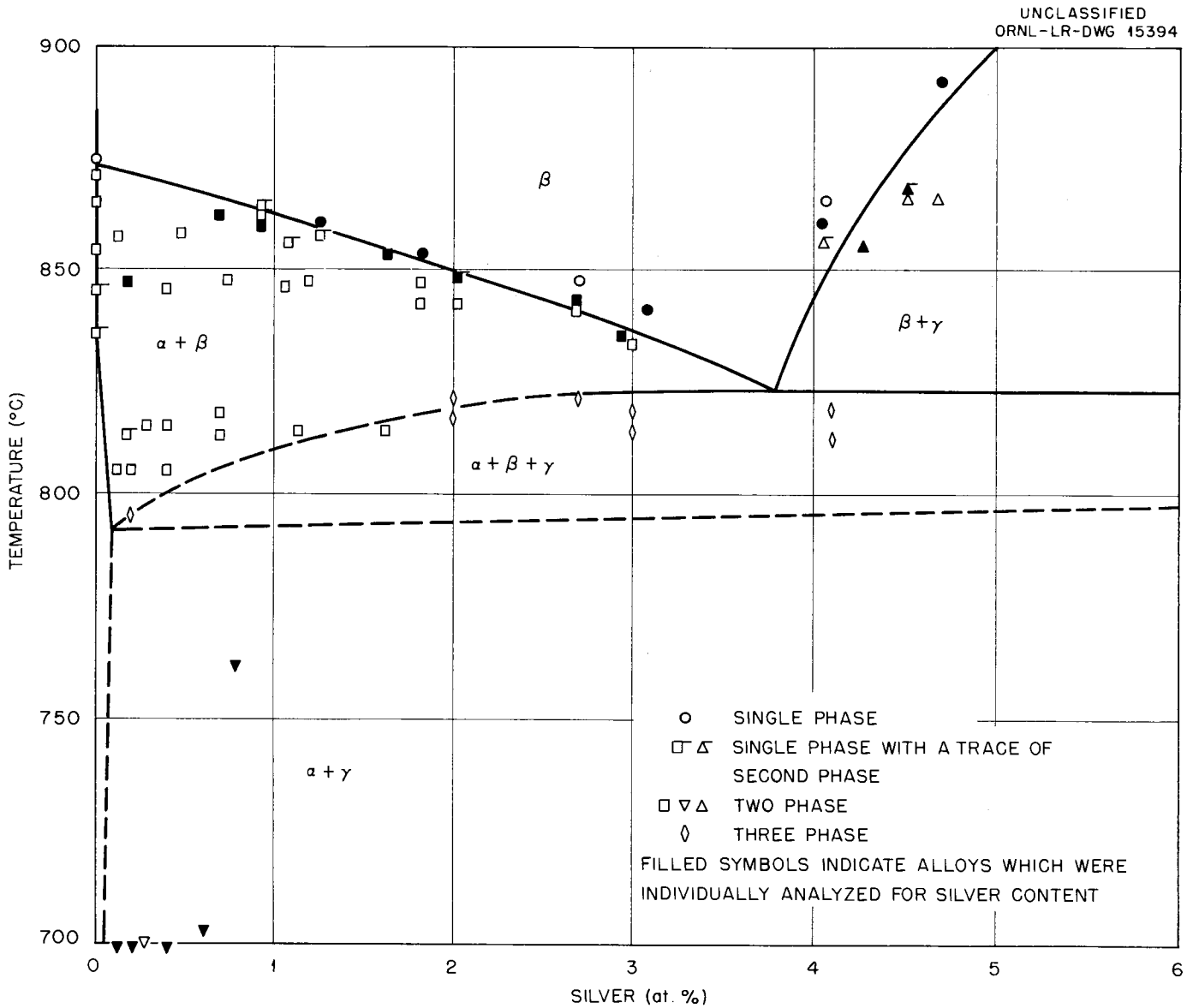

Fig. 2. Preliminary Investigation of the Eutectoid Region of the Silver–Zirconium System.

of three-phase alloys at various compositions in the temperature range 796-822°C, and two phase effects in the iodide zirconium between 835 and 873°C are indications of impurities. In order to be certain the three phase structures were not due to insufficient annealing alloys containing 3 and 4.1 at. per cent Ag were annealed at 819°C for 3 days and 69 days. The resulting microstructures contained similar proportions of the alpha, beta, and gamma phases, and thus the three phase structures after annealing for 20-30 days in this region are considered to represent equilibrium effects.

Behavior such as this can be understood in terms of an impurity which is essentially insoluble in the alpha phase and which is a eutectoid-forming element in zirconium. Since iron is an impurity of this type[7] and was present in amounts of 0.02-0.04 per cent in these alloys the effects were tentatively associated with the presence of this element, and new investigations were commenced with zirconium containing iron in the range .002-.008 per cent.

Investigation of the Alpha and Beta Phase Boundaries with Alloys of Lower Impurity Content

A final set of alloy was prepared from zirconium Batches No. 4, 5, and 6 and the phase boundaries in the vicinity of eutectoid reaction were reinvestigated by the annealing method. The results of these experiments are shown in the partial phase diagram of Fig. 3 (ORNL-LR-DWG 18989). A comparison of this diagram with that of Fig. 2 shows that considerably greater solid solubility of the alpha phase is observed in the purer alloys. On the other hand, the boundaries of the beta phase can be plotted as nearly the same curves in both diagrams. The alpha and beta phases are in equilibrium with the same phase along the $\alpha/(\alpha + \gamma)$ and $\beta/(\beta + \gamma)$ phase boundaries. It would thus appear that the free energy of the beta phase was affected much less than the alpha phase by the impurities which were varied between the preliminary and final sets of alloys.

As shown in Fig. 3 the $(\alpha + \beta + \gamma)$ region determined with the final alloys still has a temperature width of about 15°C. This region may be examined by considering the changes in the proportion of these phases as the temperature is varied, while the silver content is held constant. This is shown by the microstructures in Fig. 4, Y-16703, -16696,-16782,-17100) of an alloy with 2.1 at. per cent Ag. The proportion of beta

UNCLASSIFIED
ORNL-LR-DWG 18989

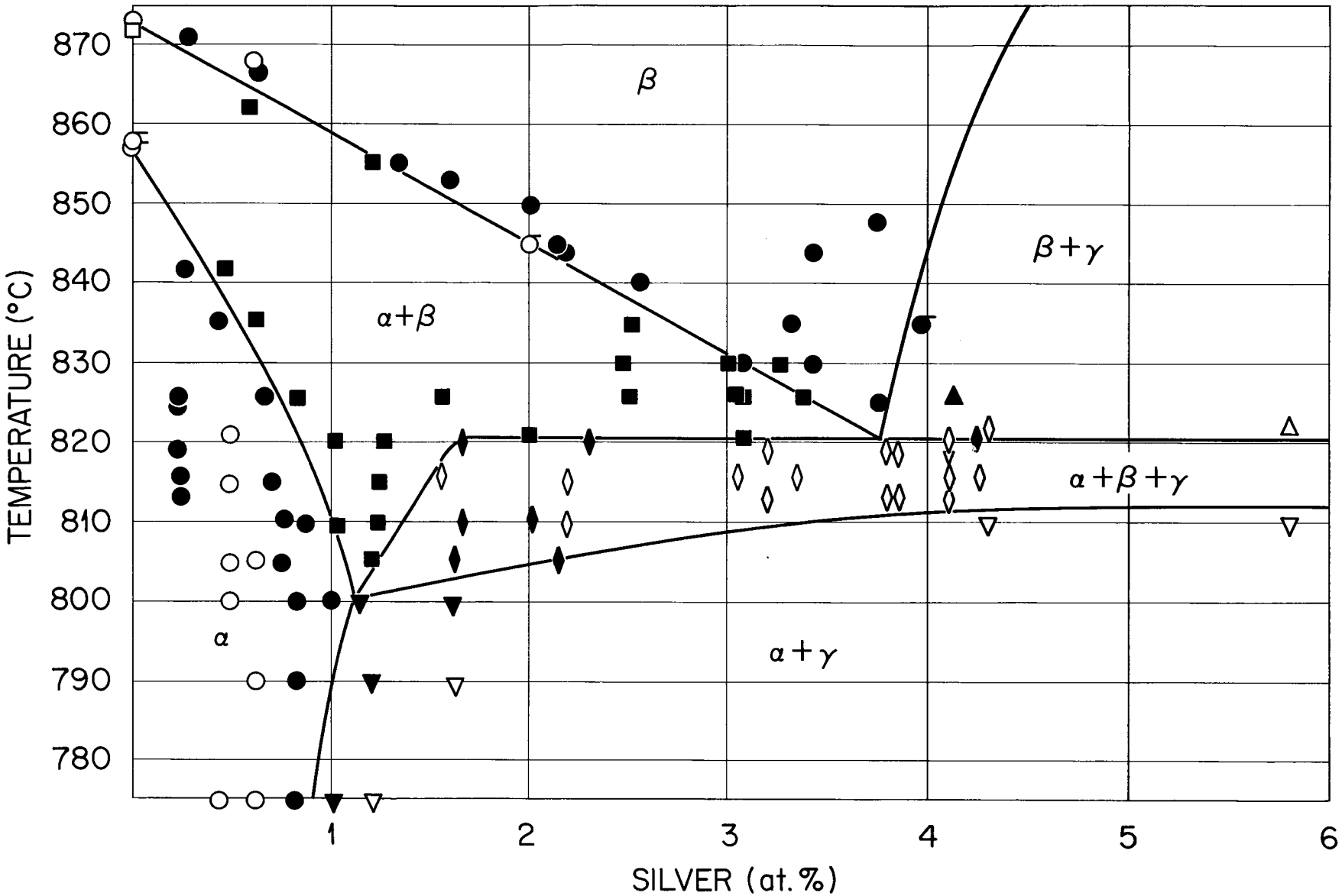

Fig. 3. Final Investigation of the Eutectoid Region of the Silver-Zirconium System.

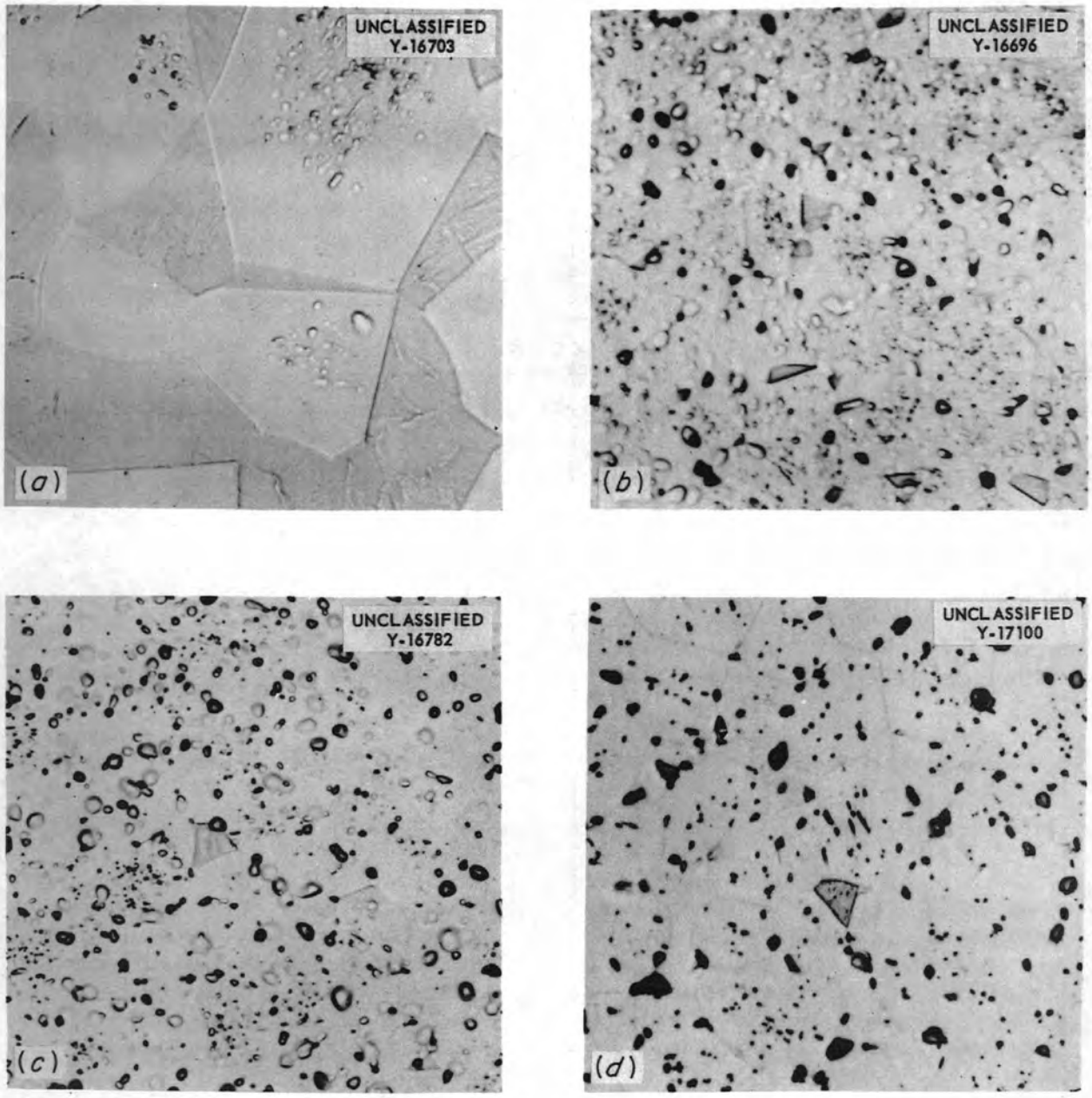

Fig. 4. Three-Phase Microstructures of Alloy Containing 2.1 at.% Silver. (*a*) Annealed 25 days at 820.1°C. 750X. (*b*) Annealed 24 days at 815.0°C. 500X. (*c*) Annealed 25 days at 809.8°C. 500X. (*d*) Annealed 29 days at 805.3°C. 750X. The gradual change with temperature in the amount of beta phase in the lower portion of the $(\alpha+\beta+\gamma)$ region is illustrated.

phase increased very slowly as the temperature is raised in the lower portion of the $(\alpha + \beta + \gamma)$ region and then rapidly in the upper part.

Only a small proportion of beta phase exists over a considerable temperature range in the lower part of this region. Hence, the possibility exists that still further reduction in beta stabilizing impurities would reduce the $(\alpha + \beta + \gamma)$ area considerably. Analysis of the 2.1 at. per cent Ag alloy showed the impurities: $\leqslant$ 3 ppm Cu 31 ppm Fe $\leqslant$ 1 ppm Mo 20 ppm Ni 6 ppm H $\leqslant$ 2 ppm W, in addition to the impurities: 115-132 ppm Hf 79 ppm C 13-222 ppm O 1-50 ppm N 7 ppm Si, present in the iodide zirconium from which the alloy was prepared. Since the known beta stabilizing elements total only 67 ppm in the above alloy, it was considered unlikely that the three phase region could be eliminated from this phase diagram using iodide-type zirconium alloys, and this three phase region was included in the final diagram.

Results of Thermal Analyses* in the Region 0-10 at. Per Cent Ag

The results of the thermal analysis of alloys prepared from Batch No. 4 zirconium are shown in Fig. 5 (ORNL-LR-DWG 16109) where they may be compared with the phase boundaries determined by the annealing method. The chemical analysis from different parts of the ingot showed a larger range of composition, as indicated by the horizontal lines in Fig. 5, than was usual for the smaller ingots used in the annealing study. Both heating and cooling results are indicated on this figure and the temperatures shown are for the beginning of the arrest in the case of the eutectoid horizontal. In the cases of the $\beta/(\alpha + \beta)$ and $\beta/(\beta + \alpha)$ boundaries the temperatures represent the end of the arrest in heating and the beginning of the arrest in cooling. The alloys with mean compositions 1.3, 2.1, 2.4, and 6.3 at. per cent Ag each showed two arrests corresponding to the phase boundary of the beta region and the eutectoid reaction respectively. The maximum arrest time for the eutectoid reaction occurred in the alloy with a mean composition 3.7 at. per cent Ag. The arrests along the $\beta/(\alpha + \beta)$ become progressively weaker with increased silver content and two of these heating arrests (Alloys 1.3 and 2.1) were quite questionable and have been

---

*The thermal analysis was performed by Mr. G. W. Cunningham while a cooperative student assigned to the Oak Ridge National Laboratory.

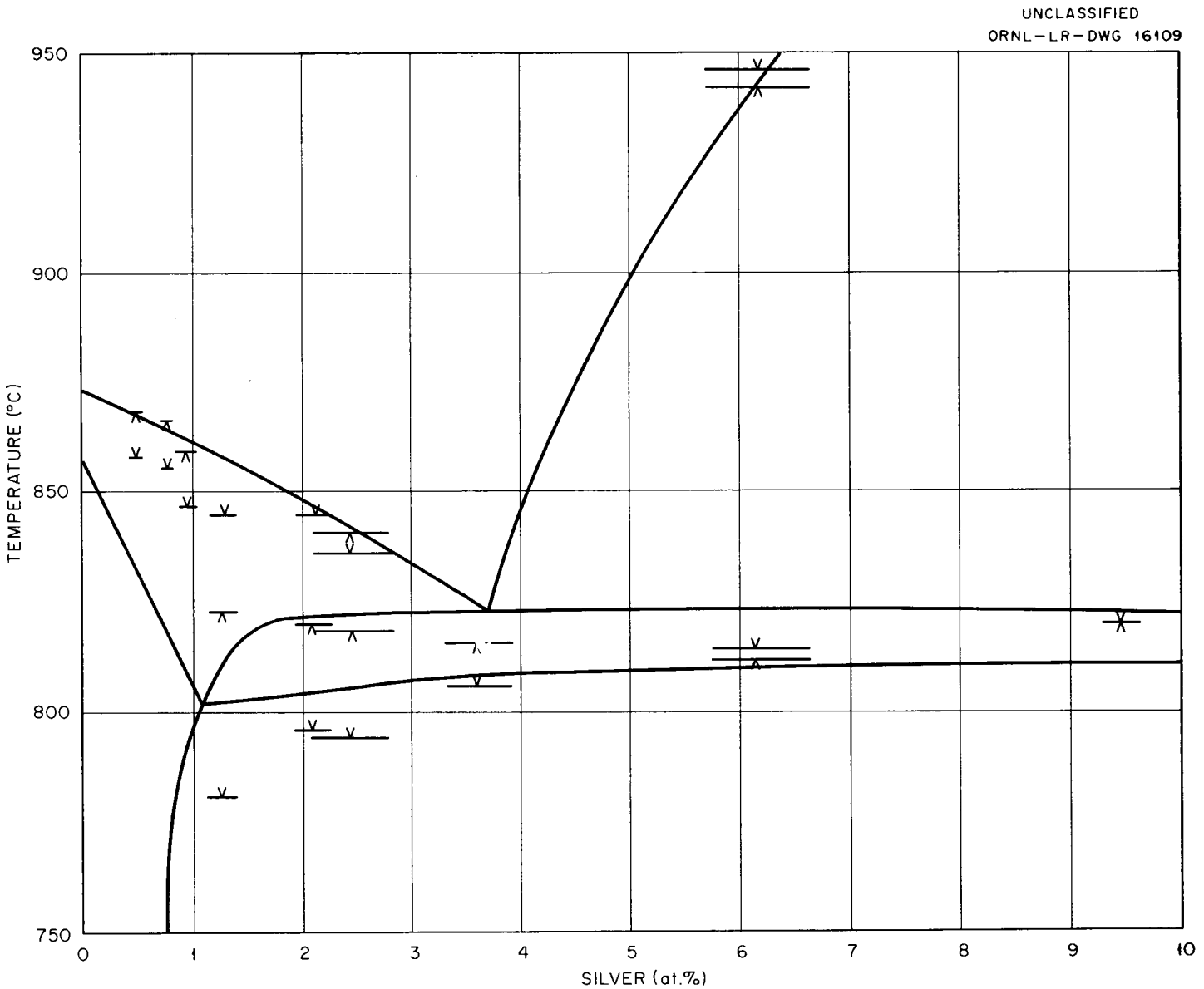

Fig. 5. Thermal Arrests in Silver-Zirconium Alloys in the Region 0-10 at.% Silver. The horizontal lines indicate both the temperature of the arrest and the range of silver composition present in each ingot. The dart symbol is used to indicate both the mean composition and whether arrest is from cooling (v) or heating (∧).

omitted from the figure. Although the thermal analysis results as indicated on Fig. 5 are only in approximate agreeement with the results from the annealing experiments, probably as a result of the compositional differences in various parts of the alloys, the eutectoid reaction and the depression of the $\beta/(\alpha + \beta)$ boundary with silver is clearly indicated by this method. Examination of the slowly cooled microstructures of these alloys showed progressively greater amounts of laminar eutectoid in the grain boundaries of the alpha phase from 0.5 at. per cent Ag to a fully eutectoid structure at 3.7 at. per cent Ag, whereas the 6.3 and 9.5 at. per cent Ag alloys consisted of progressively larger amounts of pro-eutectoid gamma crystals in a laminar eutectoid matrix.

The agreement of the above with the eutectoid reaction reported by Kemper[5]

$$\beta\ (4.7 \text{ at } \%\ \text{Ag}) \rightleftarrows \alpha\ (0.1 \text{ at.}\%\ \text{Ag}) + AgZr_2 \text{ at } 810 \pm 5°C$$

is entirely reasonable when one considers the differences which might be expected between alloys prepared from magnesium-reduced and iodide-zirconium.

The Silver-Zirconium System in the Region 6-36 At. Per Cent Ag

The results of annealing experiments to determine the phase boundaries of the beta phase at higher temperatures are shown in Fig. 6 (ORNL-LR-DWG 18988). The solubility of silver in the beta phase was found to increase from 3.8 at. per cant at 821°C to 20 at. per cent at 1191°C. Alloys within the $(\beta + \gamma)$ region during these anneals were readily detected by the presence of relatively large, gamma crystals with isothermal type boundaries. The appearance of the beta phase matrix varied considerably with composition since this phase transformed during quenching over most of the composition range. Thus quenched microstructures of beta phase vary from large grained structures with serrated grain boundaries at the lowest silver content, to martensite-like structures in the range 3-6 at. per cent Ag, and finally in the range 12-18 at. per cent Ag to structures which have the isothermal appearance of retained beta. This "retained beta" material is, however, very hard and it is thought that transformation or precipitation process has also occurred in the quenching of these compositions.

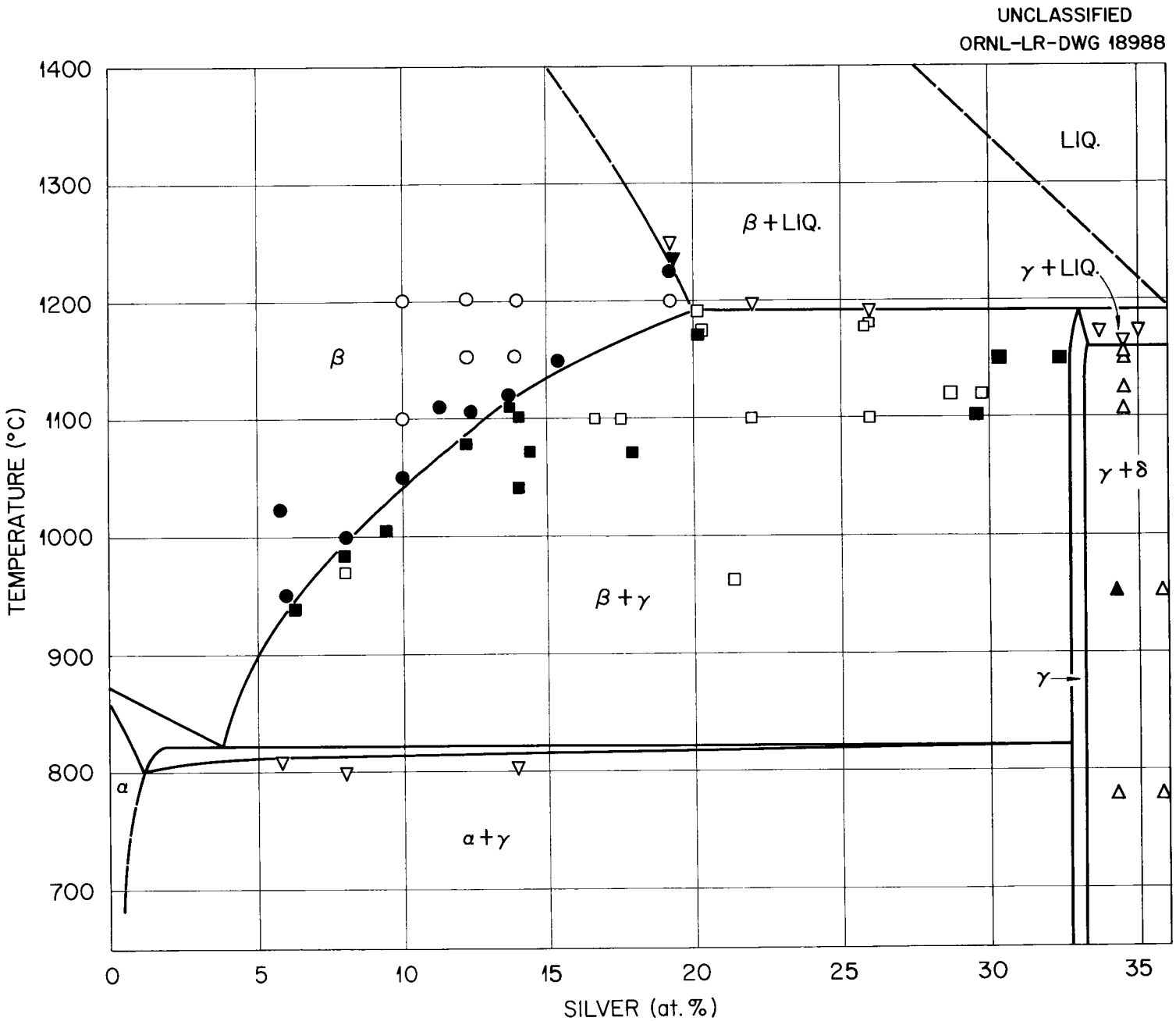

Fig. 6. The Silver-Zirconium Phase Diagram in the Region 0-36 at. % Ag.

Figure 6 also shows the constitution extended to the region of the first intermediate phase, gamma, by means of a limited investigation with alloys of higher silver content. The gamma phase is shown to form by the peritectic reaction

$$\beta \text{ (20 at \% Ag)} + \text{liquid } (\sim 36 \text{ at. \% Ag}) \rightleftarrows \gamma \text{ (33 at \% Ag)}$$

at 1191 ± 3°C. This reaction was concluded from the occurrence of ($\beta + \gamma + \delta$) peritectic-type structures in cast alloys of the compositions 25-35 at. per cent Ag and from the formation of a ($\gamma + \delta$) eutectic after melting ($\beta + \gamma$) alloys. The composition of the gamma phase was found to be between 32.4 and 34.4 at. per cent Ag at 1150°C, and although the zirconium-rich boundary of this phase was not determined at lower temperatures, the gamma phase is considered to be in equilibrium with alpha and beta phases at these temperatures. This is based on a slowly cooled alloy with 30 at. per cent Ag, comprised mainly of the gamma phase, which was observed to contain a small amount of typical ($\alpha + \gamma$) eutectoid after this treatment. X-ray examination of the above, slowly cooled specimen showed that the γ structure was that of a disordered body-centered tetragonal phase with a = 3.25 Å, c = 3.98 Å. On the other hand, a quenched specimen from the ($\gamma + \delta$) region on the silver-rich side of the phase (alloy 34.2 from 951°C) revealed a partially ordered structure that would correspond to "a" and "c" spacings twice as great as those indicated above. Further investigation of the structure of the gamma phase would therefore be desirable. This is particularly true since Karlsson[7] reported that the intermediate phase in this region was Zr_3Ag, with an ordered $AuCu_3$ type, tetragonally deformed structure. Karlsson did not completely investigate the composition of this phase because of difficulties of obtaining equilibrium in the three phase alloys, and it is of interest to note that if the type of ordering which Karlsson reported is neglected, the dimensions of the unit cell are then equivalent to those measured above, and these correspond quite well to the composition Zr_2Ag in terms of a linear atomic volume relationship between these elements. Figure 6 agrees with the earlier phase diagram of Kemper[6] in showing the first intermediate phase to be Zr_2Ag, but differs in the reaction by which this phase forms from the liquid.

The nature of the phase diagram at still higher silver contents was investigated in a preliminary fashion with alloys containing 36, 40, 50, and 66.7 at. per cent Ag. The cast structures of these alloys all contained the terminal silver phase, and in view of the existence of a (γ + δ) eutectic this suggested that an immiscible liquid region may exist above the delta phase. Such a region would also be consistent with the observation that when (δ + γ) alloys of compositions 33-35 at. per cent Ag are heated above 1160°C the delta phase melts and two eutectics, (γ + δ) and (δ + Ag), are observed in the chilled liquid.

Two annealing temperatures, 779° and 963°C, were used to investigate the phase constitution of the solid alloys. The alloy containing 50 at. per cent Ag was almost homogeneous delta phase at 963°C with only traces of chilled liquid. Thus, the delta phase corresponds to the AgZr phase reported by Raub and Engel[3] and by Karlsson[7]. An x-ray examination of this alloy revealed a tetragonal, B 11 structure in good agreement with the AgZr structure given by Karlsson.

Results with the other alloys indicated that simple two phase regions exist between the delta phase and the gamma phase and the delta phase and the silver phase without indication of additional intermediate phases. The presence of chilled liquid in the alloy containing 66.7 at. per cent Ag at 963°C was in agreement with the temperature, 955°C, given by Raub and Engel for the (Ag + δ) eutectic. The liquidus arrests of these authors rose rapidly with additions of zirconium and then formed a flat maximum at 1150-1140°C in the vicinity of 40-60 at. per cent Ag. This small variation of the arrest temperatures near the delta phase could conceivably correspond to a temperature horizontal underlying an immiscible liquid region, but further investigations are clearly needed to establish this portion of the diagram.

THE INDIUM-ZIRCONIUM SYSTEM*

Preliminary Investigation

A review of the literature at the start of the experiments indicated that no previous investigation of the indium-zirconium system had been made. A preliminary set of alloys in the range 0-26 at. per cent In were investigated by the annealing method between the temperatures 550° and 1300°C. The results are shown in Fig. 7 (ORNL-LR-DWG 16329). The alpha phase was found to form by a peritectoid reaction, β (9.5 at. % In) + γ (22.4 at. % In) $\rightleftarrows$ α (10.6 at. % In), at 1050° ± 30°C. The phase designation, γ, refers to the first intermediate phase, which exists over the composition range 22.4 to 26.1 at. % In, and may extend to higher indium contents which were not investigated. X-ray examination of this phase showed that the crystal structure was the face-centered cubic, similar to that of copper, with a = 4.45 ± 0.01 Å. Strong, binding forces are indicated in this phase since the mean atomic volume is significantly contracted compared to that indicated by Vegard's Law, even where allowance is made for the probable state of incomplete ionization in pure indium metal. Alloys in the ($\alpha + \gamma$) region were examined by x-ray diffraction and no other intermediate phases were observed. Since the α/β phase boundaries were observed to increase in temperature, the effect of indium on the alpha and beta phases is to lower the relative free energy of the alpha phase compared with that of the beta phase.

The ($\alpha + \beta + \gamma$) region indicated on Fig. 7 (ORNL-LR-DWG 16329) is hypothetical since the temperature intervals in the preliminary experiment were not sufficiently close to investigate this region. The boundary between the alpha and the ($\alpha + \gamma$) region was drawn on the basis of the occurrence of a characteristic ($\alpha + \gamma$) microstructure shown in Fig. 8a. An insoluble impurity phase, which was not dependent upon the indium content, appeared in many of the alpha alloys and was not considered in the construction of the diagram. This phase is illustrated by the microstructure given in Fig. 8b.

---

*The authors wish to acknowledge the assistance of Prof. G. W. Boyd during the preliminary experiments and of Dr. W. K. Noyce during the final experiments in the Indium-Zirconium system while participants in the summer research program at this Laboratory.

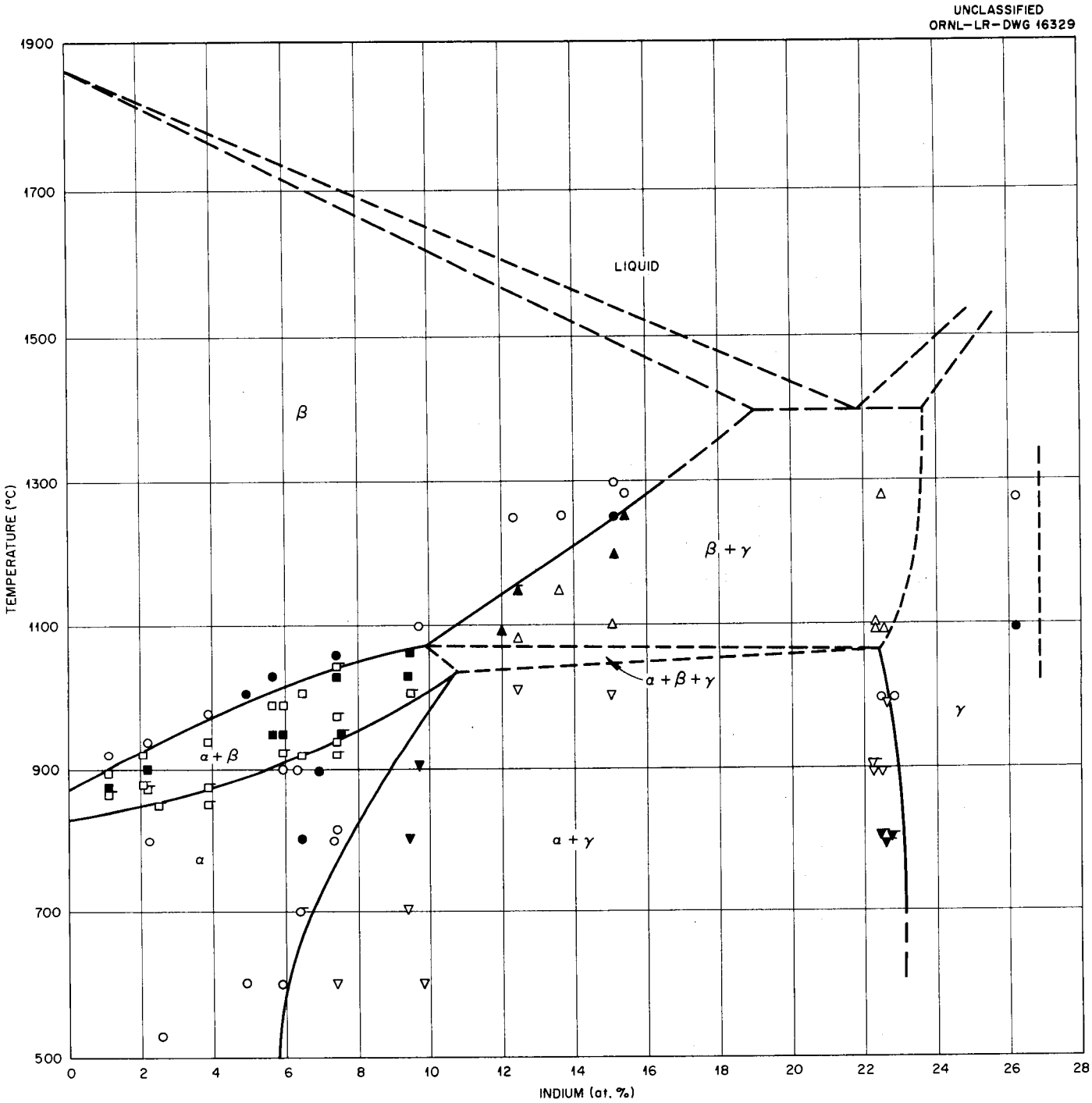

Fig. 7. Preliminary Investigation of the Indium–Zirconium Phase Diagram in the Region 0–28 at. % Indium.

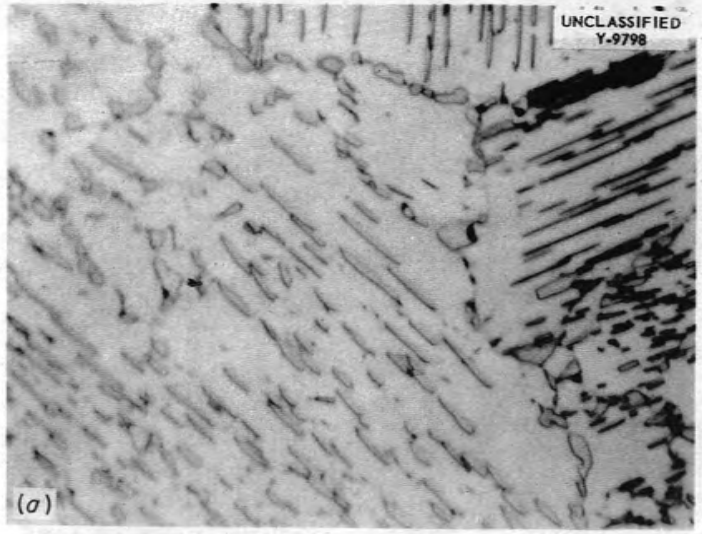

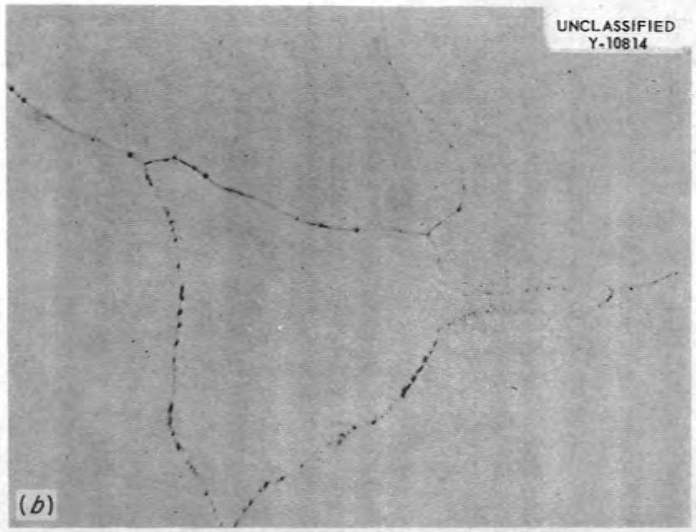

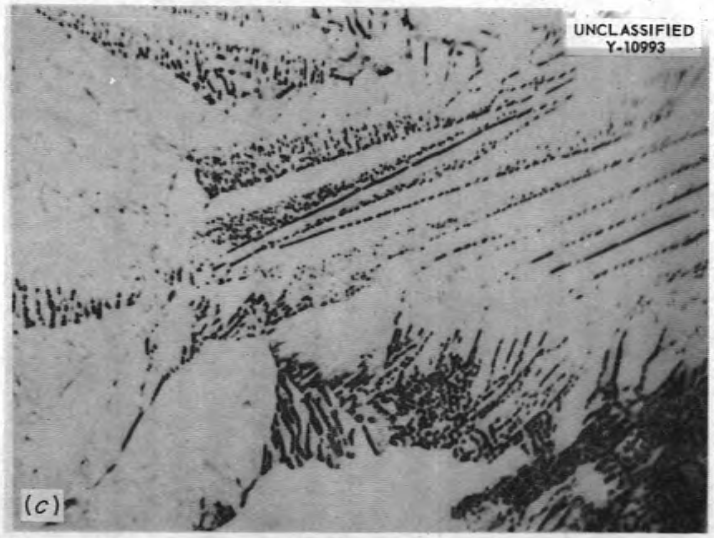

Fig. 8. Microstructures of In-Zr Alloys. (*a*) 9.4 at.% Indium, 600°C, needle-like gamma phase in alpha matrix, 1300X. (*b*) 5.9 at.% Indium, 780°C, impurity phase in boundaries of alpha grains, 500X. (*c*) 23 at.% Indium, as-cast structure, ($\beta+\gamma$) eutectic in primary crystals of gamma phase, 1500X.

The microstructures of the cast indium-zirconium alloys were complicated in appearance by transformation and precipitation effects. A eutectic is believed to be present, however, in the vicinity of 21-22 at. per cent indium on the basis of cast microstructures. Figure 8c illustrates this eutectic between primary gamma crystals in a hypereutectic alloy containing 23 at. per cent In.

Investigation with Alloys of Lower Impurity Content

As indicated in the section on experimental procedure a final set of alloys were prepared with greater purity. The annealing results from these alloys are shown in Fig. 9 (ORNL-LR-DWG 18987). The α/β phase boundaries are much closer together in the improved alloys. As a consequence, the agreement of the final alloys with the lever rule across the $(\alpha + \beta)$ region was much better than in the preliminary work. This is illustrated by Fig. 10 (ORNL-LR-DWG 8133), which shows the volume proportion beta phase as a function of indium content in this region at 900°C.

The peritectoid reaction occurred at a lower temperature, 1003° ± 20°C, in these alloys with the composition indicated by the relation,

$$\beta\ (9.3 \text{ at. \% In}) + \gamma\ (22.4 \text{ at. \% In}) \rightleftarrows \alpha\ (10.1 \text{ at. \% In}).$$

A three phase region $(\alpha + \beta + \gamma)$ occurred in the vicinity of this reaction. This was in spite of the reduction of the impurities in these alloys to quite low levels, as indicated in Table III, compared to the usual impurities in the iodide-zirconium. The results for the $\beta/(\beta + \gamma)$ boundary agree within the experimental accuracy with the preliminary results and suggest that this boundary is not as sensitive to impurities as the α/β boundaries. The $\alpha/(\alpha + \gamma)$ boundary also agrees reasonably with the preliminary boundary, but in the final alloys the amount of insoluble impurity phase present in the alpha region was greatly reduced.

UNCLASSIFIED
ORNL-LR-DWG 18987

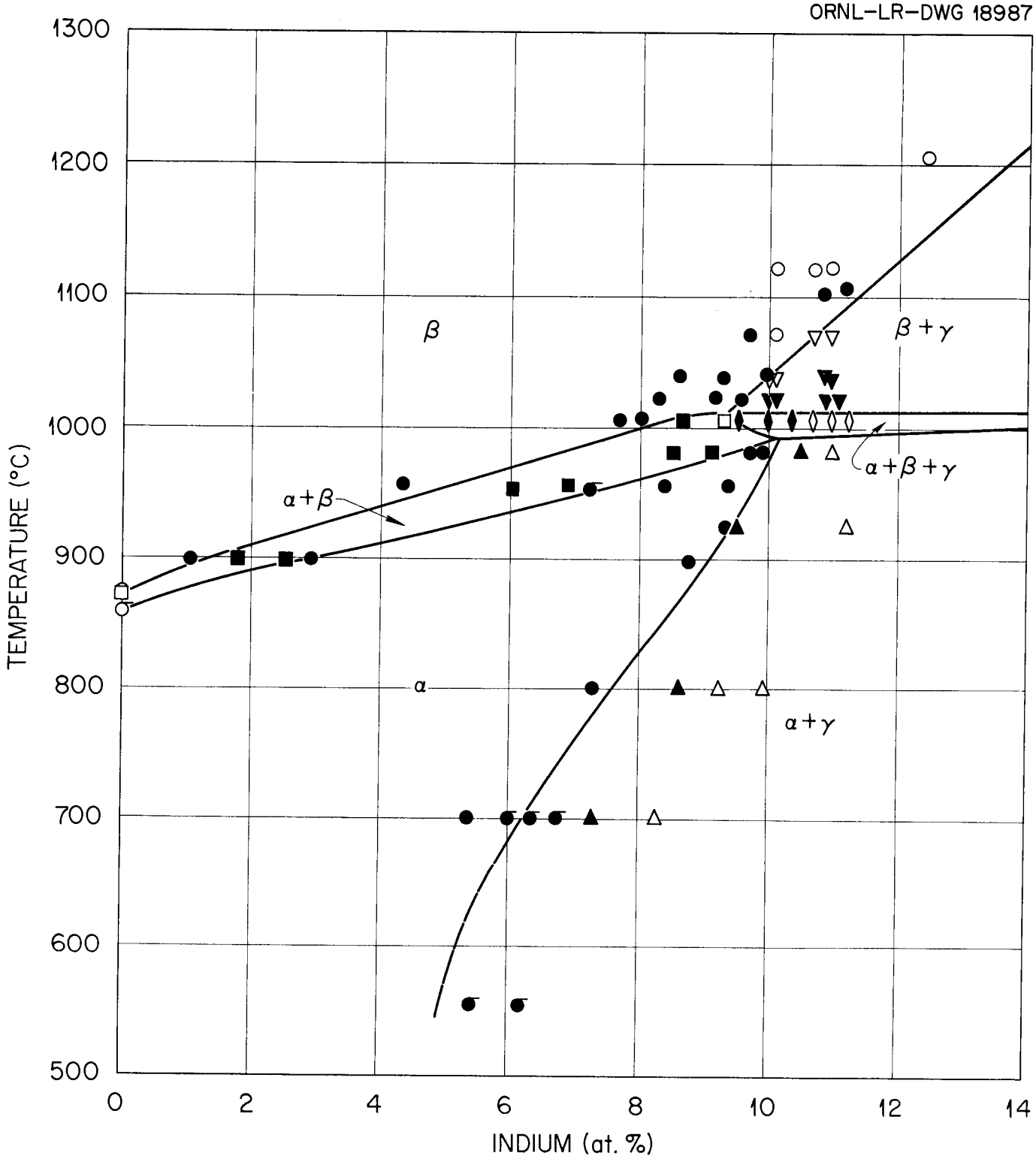

Fig. 9. Final Investigation of the Indium–Zirconium Phase Diagram in the Region 0–13 at. % Indium.

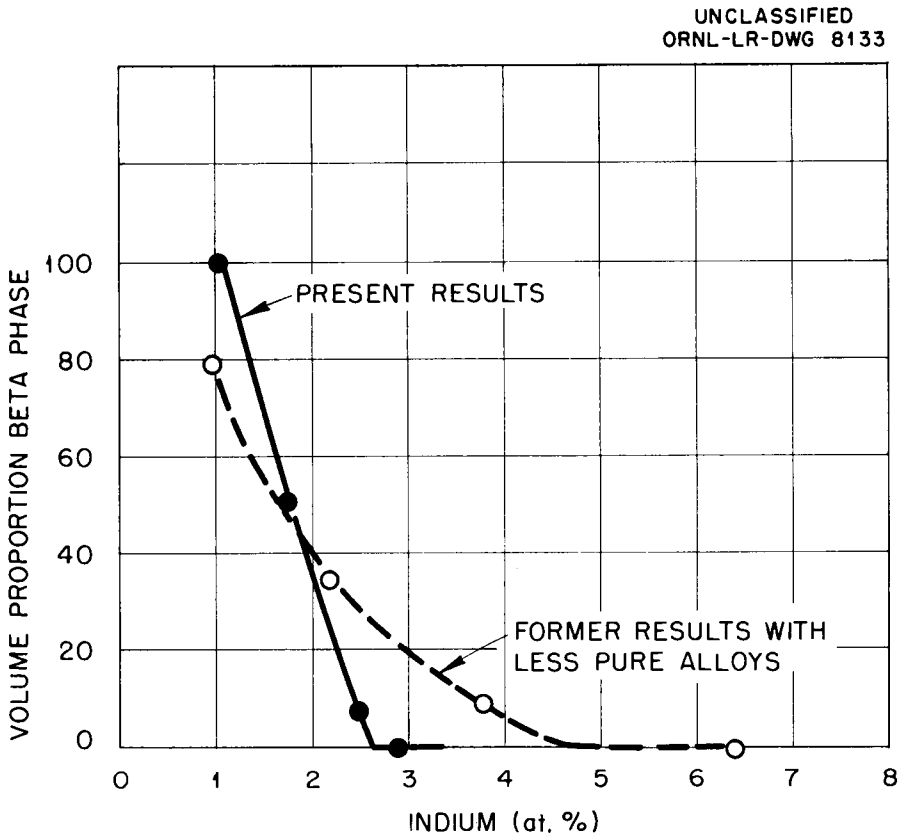

Fig. 10. Effect of Impurities on the Variation of the Volume Proportion of Alpha and Beta Phases in the ($\alpha + \beta$) Regions at 900°C.

THE ANTIMONY-ZIRCONIUM SYSTEM

Literature

The first investigation of the antimony-zirconium alloys was made by Russi and Wilhelm[8] who showed that a eutectic reaction occured in the zirconium-rich end of this system between the first intermediate phase, Zr_2Sb, and β-zirconium solid solution of approximately 11 at. per cent Sb. The composition of this eutectic was found to be 17.5 at. per cent Sb with a temperature of 1430°C. By means of thermal analyses on magnesium-reduced zirconium alloys, Russi and Wilhelm found evidence for an increase in the temperature of the zirconium transition with additions of antimony but the details of this effect were not fully determined.

Preliminary Investigation*

The present study of this system, with preliminary alloys of iodide-zirconium, was made in the region 0-5 at. per cent Sb and between the temperatures 800° and 1300°C. The partial equilibrium diagram determined by the annealing method is given in Fig. 11 (ORNL-LR-DWG 18983). The solid solubility of the beta phase decreased with temperature and at temperatures in the vicinity of 869°C a peritectoid reaction

$$\beta\ (\sim 0.1 \text{ at. \% Sb}) + \gamma\ (Zr_2Sb) \rightleftarrows \alpha\ (\sim 0.7 \text{ at. \% Sb})$$

occurred. The (α + β) region has been idealized on this diagram since only two alloys at two temperatures were investigated and subsequent work showed that with the Batch No. 3 zirconium from which these alloys were prepared, had a wide transition range (See Fig. 2).

This region was reinvestigated with alloys made with zirconium of Batches No. 4 and 6 but with the less favorable casting and outgassing conditions, usually present in the preliminary studies. The results of this experiment are shown in Fig. 12 (ORNL-LR-DWG 16274). The peritectoid reaction occurred at higher temperatures, 874°-881°C, in these alloys, presumably due to the lower iron content of the iodide-zirconium used.

---

*The authors wish to acknowledge the assistance of Dr. W. M. Spicer during the preliminary experiments on the antimony-zirconium system.

UNCLASSIFIED
ORNL-LR-DWG 18983

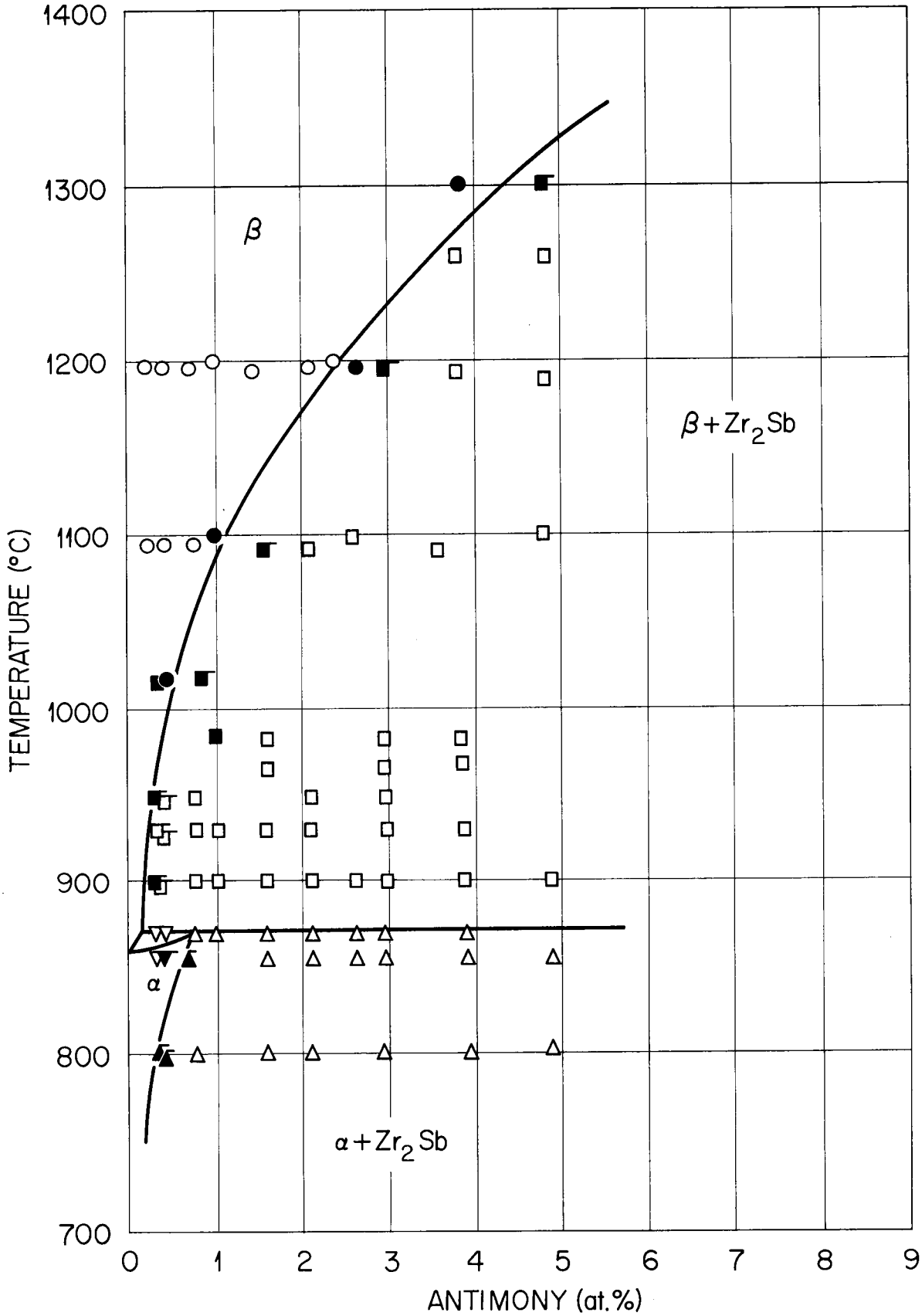

Fig. 11. Preliminary Investigation of the Antimony – Zirconium Phase Diagram in the Region 0 – 6 at. % Antimony.

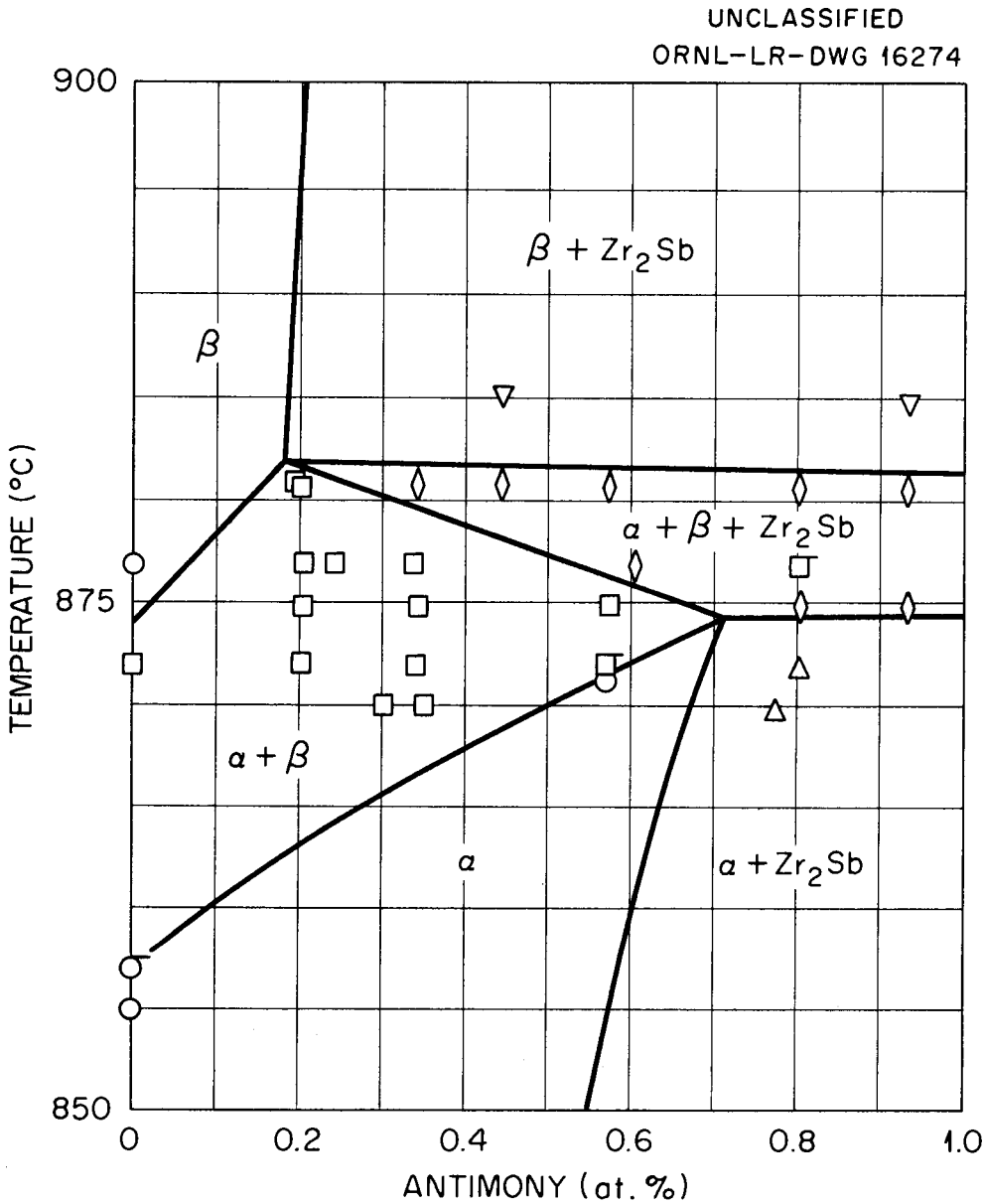

Fig. 12. Peritectoid Region of the Antimony–Zirconium Phase Diagram, According to the Preliminary Investigation.

Final Investigation

The final alloys in the range 0-0.8 at. per cent Sb were prepared under better casting conditions, corresponding to the final alloys in the other two systems. The iodide-zirconium used was Batch No. 6. The results of this experiment are shown in Fig. 13 (ORNL-LR-DWG 16272). The solid solubility of antimony in alpha zirconium was found to decrease from 0.48 at. per cent at 869°C to < .1 at. per cent at 760°C. The ($\alpha + \beta$) region rose from the 857-873°C range for pure zirconium to 869-880°C at 0.48 at. per cent Sb.

Although the impurities, as indicated by analyses given in Table III and by the extrapolated hardness of pure zirconium from these alloys (58-65 VPN), were quite low, compared to the impurities usually present in iodide-zirconium, the effect of antimony on the transition temperature was only approximately determined. The occurrence of the ($\alpha + \beta$) temperature range in pure zirconium and the ($\alpha + \beta + \gamma$) region in the phase diagram above 0.5 at. per cent Sb prevented a more accurate determination. The lower hardness of these alloys compared with the preliminary alloys is presumably a result of lower alpha stabilizing impurities. This had the effect shown by comparison of Fig. 12 and Fig. 13 of increasing the solubility of antimony in the beta phase to 0.5 at. per cent Sb at the peritectoid temperature in the final diagram.

UNCLASSIFIED
ORNL-LR-DWG 16272

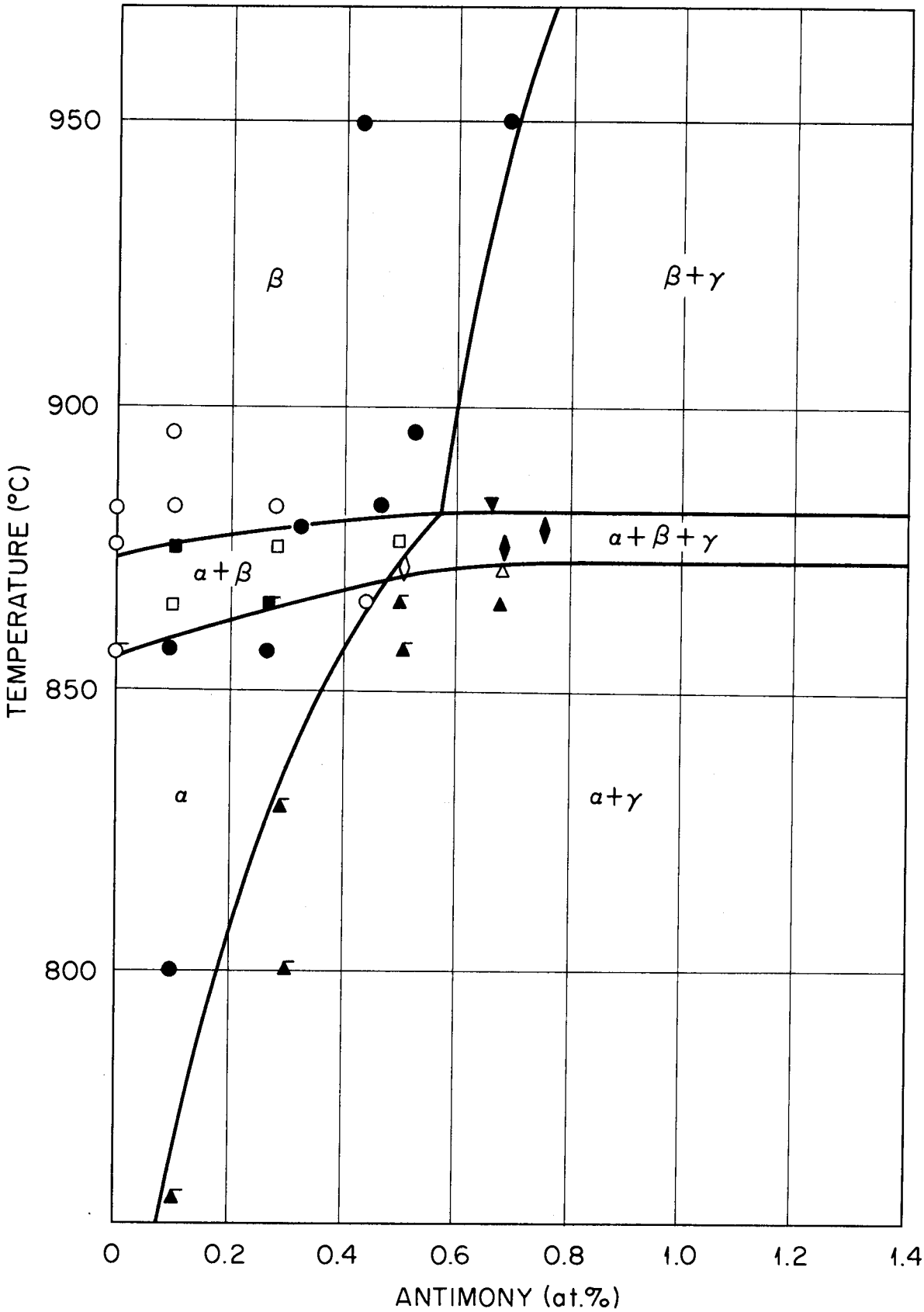

Fig. 13. Final Investigation of the Peritectoid Region of the Antimony-Zirconium System.

FACTORS AFFECTING THE α/β BOUNDARIES OF ZIRCONIUM AND TITANIUM

The experimental α/β boundaries of the zirconium-silver, zirconium-indium and zirconium-antimony systems may be compared to other zirconium systems in the literature[9] and these boundaries will be found to vary with the position of the solute in the Periodic Table. For example, when zirconium is alloyed with transition element solutes to the right in the Periodic Table and including the elements of Group IB, the α/β boundaries are depressed; whereas, when the solute is from Groups IIIB, IVB, or VB the α/β boundaries are elevated. To a reasonable degree of correctness, these effects can be expressed as a valency rule, the nature of which is illustrated in Fig. 14 (ORNL-LR-DWG 18986) for three zirconium systems[10].

The phase boundaries of titanium alloys are similar to those of zirconium alloys and, with exception of the anomalous solutes Si, Sn, and Pb, the same general behavior is found for titanium systems. The effects of aluminum and copper on the α/β boundaries of titanium are shown in Fig. 14. Correlations of the allotropic phase boundaries to the valency and the position of the solute on the Periodic Table are not unique to Group IVA solvents, but are known to be true for other elements such as iron[11] and cobalt[12]. As an example of the effects in these elements, the data of Koster[12] showing the effect of copper, gallium, and arsenic on the ϵ/γ boundaries of cobalt have been plotted in Fig. 14 and resemble closely those encountered in zirconium alloys.

Because of the special conditions which govern the free energy of metallic phases the phase boundaries are often found to be functions of electron concentration. If this is true in the present case, the opposite effects of the univalent and trivalent solutes on the temperatures of the allotropic transitions of zirconium and titanium suggest that these elements are divalent in the metallic state.* The hypothesis can be tested by assuming the divalency and plotting the positions of the known zirconium systems with B-sub group solutes as a function of electron concentration. The results are shown in Fig. 15 (ORNL-LR-DWG 16106). In this graph the horizontal bars represent the experimental width of the $(\alpha + \beta)$ region at some

---

*It is highly probable that four electrons occupy overlapping d and s bands in Zr and Ti, but it may be that only two of these are important in the present phenomenon. This will be discussed later.

UNCLASSIFIED
ORNL-LR-DWG 18986

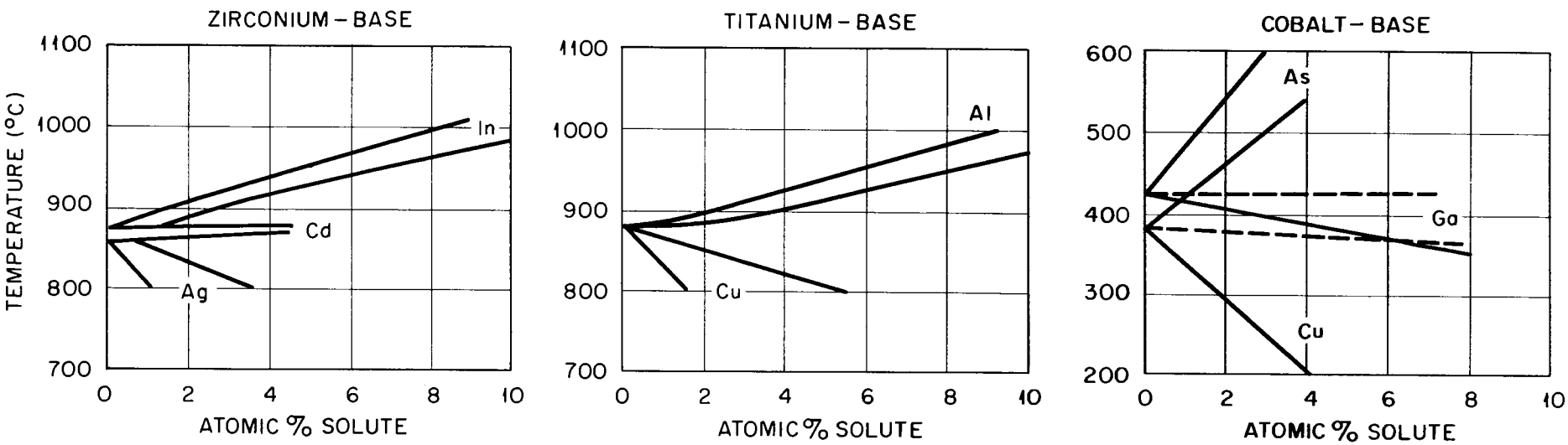

Fig. 14. Position of the Phase Boundaries Between the Allotropic Forms of Zirconium, Titanium, and Cobalt with Solutes of Different Valency.

UNCLASSIFIED
ORNL-LR-DWG 16106

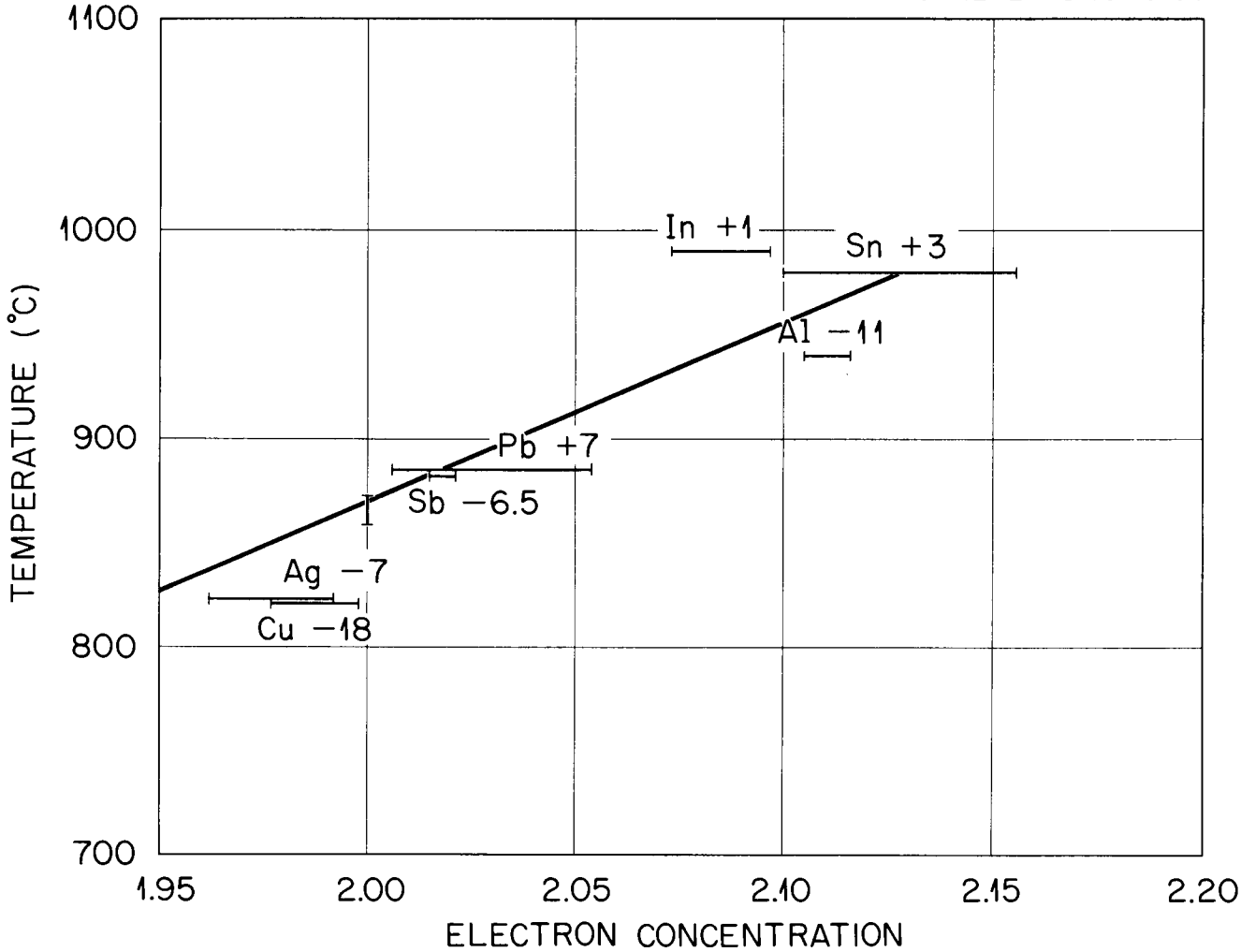

Fig. 15. The Variation of the Temperature of the α/β Phase Boundaries in Zirconium Systems with Electron Concentration. The horizontal bars represent electron concentration limits within which the constitution is $(\alpha+\beta)$ at the particular temperature indicated. The numbers represent atomic size factors.

particular temperature selected from the phase diagram. For simplicity only one temperature is shown, usually near the temperature of the eutectoid or peritectoid reaction where the impurities in the alloys would be expected to have a smaller effect. Although the agreement of these zirconium systems with a common linear relationship is fairly approximate an important effect of electron concentration is indicated.

When the positions of the $\alpha + \beta$ regions of the known titanium alloy systems[13] with B-sub group elements are plotted in the same way, as indicated in Fig. 16 (ORNL-LR-DWG 16107), the same behavior is found for only part of these systems and it is apparent that an additional factor is affecting these phase diagrams. In common with observations which have been made in other alloy studies[1] a size factor effect is often present which obscures the valency relationship. For this reason the atomic size factors have been shown on these figures for each alloy system. These numbers are based on the percentage difference in minimum interatomic distances in the pure elements concerned except for the solutes aluminum, indium, tin, and lead. The sizes of these elements are thought to be irregular in their pure element form, and the approximate atomic diameters, obtained by Vegard's Law extrapolation of the lattice spacings of dilute alloys in which these elements were solutes,[14, 15, 16] have been used for the present purpose.

In both Fig. 15 and 16 the larger size factors tend to depress the phase boundaries below the straight line, representing a linear dependence upon electron concentration. This result may be understood, because the body-centered cubic beta phase is less densely packed, has lower coordination number, and, at least in the case of zirconium, has elastic moduli of smaller magnitude than the hexagonal, alpha phase. Thus, from examination of Figs. 15 and 16 the second important effect appears to be that of size factor, and if this is accepted, the previously anomalous behavior of Si, Sn and Pb in titanium can be explained in this way. On the other hand, if the closest distances in the elements are used throughout in evaluating size factors, the size relationship is not importantly altered except for Ti-Sn which remains anomalous in this case.

For a full understanding of the phase boundaries it would be desirable to express concentration in terms not alone of temperature but also of the energies, entropies, and specific heats involved. Data are not now available which would

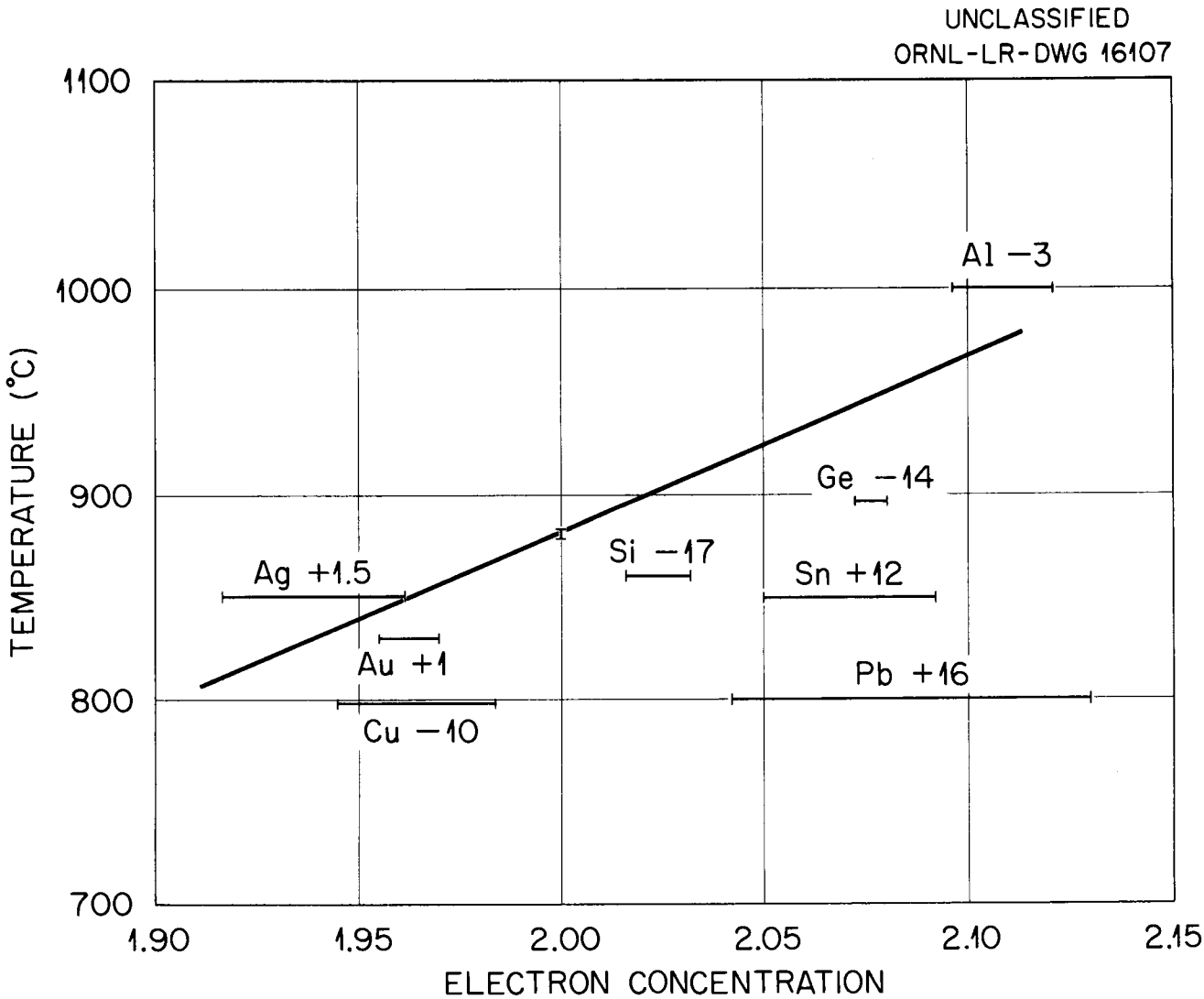

Fig. 16. The Variation of the Temperature of the α/β Phase Boundaries in Titanium Systems with Electron Concentration. The horizontal bars represent electron concentration limits within which the constitution is $(\alpha + \beta)$ at the particular temperature indicated. The numbers represent atomic size factors.

permit this to be done in detail and the calculation of such quantities cannot be carried out with sufficient accuracy to be useful. It is possible, however, to derive general equations for concentration as a function of energy, entropy, specific heat, and temperature. Such equations are helpful in two ways. First they serve as guide in discussing the α/β boundaries. Second and more important, they indicate additional experiments which must be performed if a fuller understanding of these boundaries is to be obtained.

THERMODYNAMIC EXPRESSION OF THE PHASE BOUNDARIES

When two terminal alloy phases are present in a binary phase diagram as a result of an allotropic transition in the solvent metal, it can then be shown from the usual conditions for equilibrium and the following equation[x] for the free energy of an alloy phase,

$$F_\alpha = E_{o\alpha} - \int_o^T dT \int_o^T C_\alpha \frac{dT}{T} + KT\left(x_\alpha \ln x_\alpha + (1-x_\alpha)\ln(1-x_\alpha)\right),$$

that the compositions of the phase boundaries, x_α and x_β, are given by[+]

$$x_\alpha = \frac{e^{-L} - 1}{e^{-N} - 1} \qquad (1)$$

$$x_\beta = \frac{e^{L} - 1}{e^{N} - 1}$$

when

$$L = \frac{1}{kT}\left[\begin{array}{l} \lambda_c^o\left({}^{T}/_{T_c} - 1\right) - \int_{T_c}^{T} \Delta C^o dT + T\int_{T_c}^{T} \Delta C^o \frac{dT}{T} \\ + x_\beta\left(\dot{E}_{o\beta} - \dot{f}(C_\beta,T)\right) - E_{o\beta}(x) + f_x(C_\beta,T) \\ - x_\alpha\left(\dot{E}_{o\alpha} - \dot{f}(C_\alpha,T)\right) + E_{o\alpha}(x) - f_x(C_\alpha,T) \end{array}\right]$$

$$N = \frac{1}{kT}\left[\Delta\dot{E}_o - \dot{f}(\Delta C,T)\right]$$

In the above, $f(C,T)$ is convenient notation for the integral $\int_o^T dT \int_o^T C\frac{dT}{T}$. E_α and E_β are the energies of the alpha and beta phases, respectively. C_α and C_β are the specific heats at constant volume. λ_c^o is the latent heat of the pure solvent transition at the temperature T_c. The dot symbol indicates differentiation with respect to x_α or x_β. The superscript ^{o} indicates pure solvent, the subscript $_o$ indicates 0^oK. The Δ symbol indicates difference in the sense beta minus alpha

---

[x] The discussion will be essentially unaltered if the Gibbs free energy and a system of constant pressure is assumed instead of the Helmholtz free energy and a system of constant volume. In this case, $H_o = E_o + PV_o$ is substituted for E_o and C_p for C_V.

[+] We are indebted to Dr. G. D. Kneip, Jr. for pointing out that a similar relation has also been given by H. Jones[17] for the solidus and liquidus boundaries of alloys.

and $E_{o\beta}(x)$ and $f_x(C_\beta,T)$ refer to $E_{o\beta} - E^o_{o\beta}$ and $f(C_\beta,T) - f(C^o_\beta,T)$, respectively.

Thus with the approximations of constant volume and ideal mixing entropy in both phases, the phase boundaries can be calculated from a knowledge of the effects of various solute elements upon the energy at absolute zero of temperature and upon the specific heats. For the present some additional approximations are desirable. The simpliest approximation is the E_o and C of each phase depend upon composition in the dilute alloy region in such a manner that $\ddot{E}_o$ and $\ddot{C}$ vanish. The exponent L then becomes

$$L = \frac{1}{kT}\left[\lambda^o_c(T/T_c - 1) - \int_{T_c}^{T}\Delta C^o\, dT + T\int_{T_c}^{T}\Delta C^o\,\frac{dT}{T}\right].$$

For values of T not too greatly different than T_c, the term $-\int_{T_c}^{T}\Delta C^o\, dT + T\int_{T_c}^{T}\Delta C^o\,\frac{dT}{T}$ would be expected on the basis of extrapolations of the specific heat measurements in the pure solvent[18,19,20,21], to be small compared to the latent heat term. L then becomes approximately $\frac{1}{kT}\lambda^o_c(T/T_c - 1)$. The other exponent N depends upon both the rates of change of the relative energy at absolute zero of temperature and the relative specific heats of the two alloy phases with respect to composition. Following Jones[17], the approximation is made that the effect of alloying upon the specific heats is smaller than the effect upon the energy at absolute zero. Thus $\Delta\dot{C}$ is neglected entirely and N is given approximately by $\Delta\dot{E}_o/kT$.

Since every term is now known except $\Delta\dot{E}$ the experimental boundaries of an alloy system may be used to solve the equation (1) for $\Delta\dot{E}$ at various temperatures. This has been done for the $\alpha/(\alpha + \beta)$ and $\beta/(\alpha + \beta)$ boundaries of the Ag-Zr and In-Zr systems, and the results are shown in Fig. 17 (ORNL-LR-DWG 18985). The relative change in energy is reasonably constant in magnitude with variations in temperature, and hence with solute composition; for the $\alpha/(\alpha + \beta)$ and $\beta/(\alpha + \beta)$ boundaries of In-Zr and the $\beta/(\alpha + \beta)$ boundary of Ag-Zr. For the $\alpha/(\alpha + \beta)$ boundary of Ag-Zr and for temperatures near T_c in both systems, the results are variable and of different magnitudes. The latter regions, however, are those most strongly affected by minor impurities in the alloys. Estimates of the size of these impurity effects indicate that they are sufficient to explain these deviations of the relative energy changes. Thus the agreement with the approximations will be considered to be reasonable.

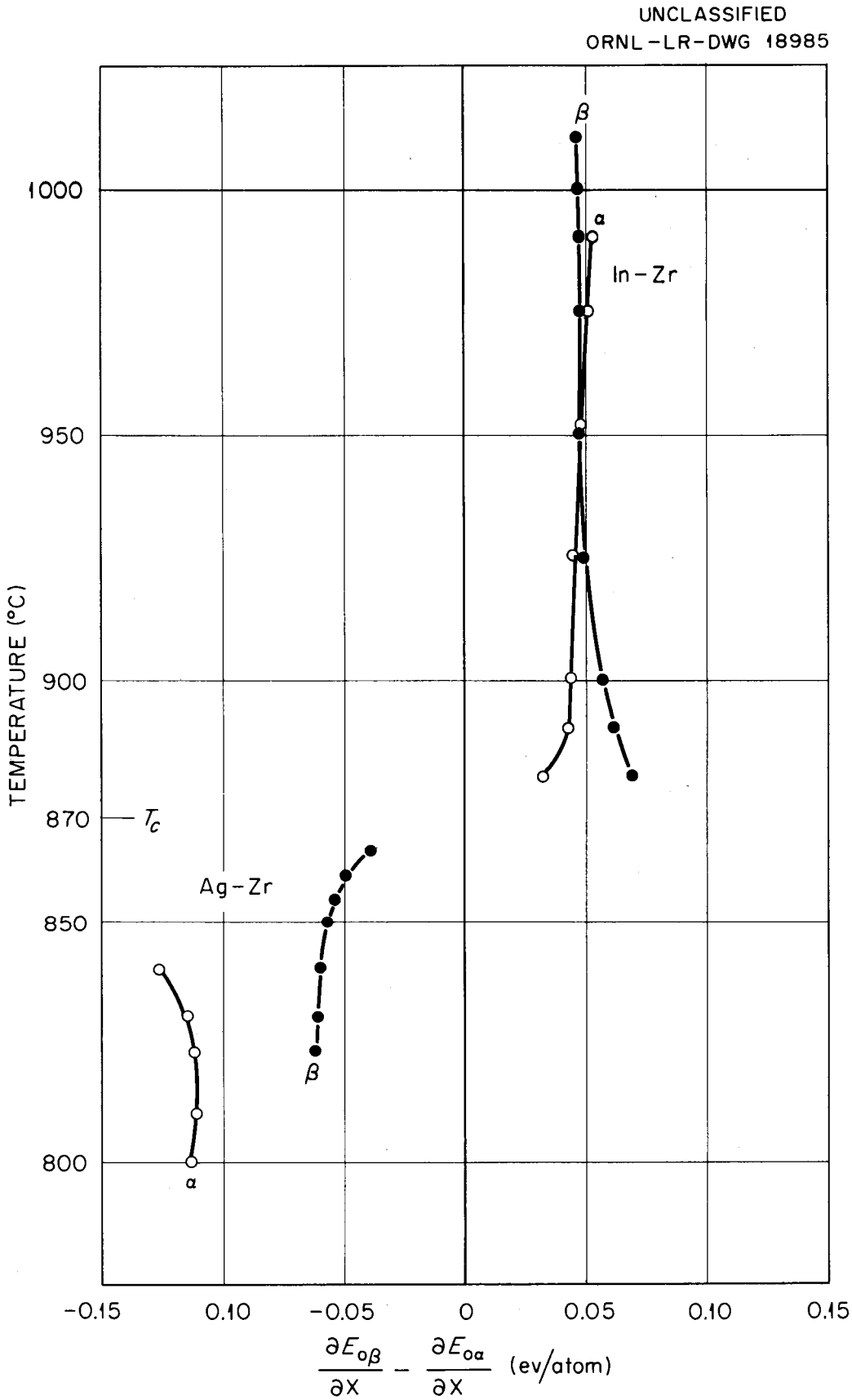

Fig. 17. Relative Energy Change with Alloying of the Alpha and Beta Phases Calculated from the $\alpha/(\alpha+\beta)$ and $\beta(\alpha+\beta)$ Phase Boundaries of the Ag-Zr and In-Zr Systems.

APPROXIMATE METHODS FOR DERIVING ENERGY PARAMETERS FROM THE ALLOY SYSTEMS

In view of the above, a more approximate procedure will be adopted for further comparison of the different alloy systems. The first few terms of a series expansion of the exponentials in expressions (1) are substituted in these expressions, and a mean value, x_m, of the phase boundary compositions, x_α and x_β, derived.

$$x_m \simeq \frac{\lambda_c^o \left(T/T_c - 1\right)}{\Delta^{\cdot}E_o} \qquad (2)$$

This relation may also be expressed in terms of the other composition variable n, the electron concentration,

$$n_m - n^o \simeq \frac{\Delta S_c^o \left(T - T_c\right)}{\Delta^n E_o} \qquad (3)$$

Here ΔS_c^o, or λ_c^o/T_c, is the entropy change during the transition in the pure solvent, $\Delta^n E_o$ is the difference $\frac{\partial}{\partial n}(E_{o\beta} - E_{o\alpha})$. The relationship between the electron concentration and the mole fraction solute is given by $n = n^o + x(\Delta n)$ where Δn is the difference in valency of the solute and the solvent.

In terms of the earlier assumption that $\ddot{E}_{o\alpha}$ and $\ddot{E}_{o\beta}$ vanish, the quantity $\Delta^n E_o$ will be constant with respect to variations in composition. If in addition $\Delta^n E_o$ has the same value in different alloy systems, the relation (3) results in a common linear behavior between the mean electron concentration of the phase boundaries and temperature, such as was suggested earlier by the straight lines on Fig. 15 and 16.

Equation (2) may now be used to derive approximate values of $\Delta^{\cdot}E$ for each system, using the phase boundary data at the particular temperatures shown in Figs. 15 and 16. The results are given for both zirconium and titanium alloys in Table IV. If these values of $\Delta^{\cdot}E$ are now regarded as dependent solely upon a term proportional to the valency difference and a term related to the size factor, the data can be fitted by least squares to a linear combination of the type

$$\Delta^{\cdot}E = K_1 \Delta n + K_2 S$$

representing the simplest possible dependence upon these factors, where S represents the square of the size factors for reasons which will be explained below. The constants obtained for the zirconium alloys were $K_1 = 0.032$ e.v./electron and

TABLE IV

$\Delta^{\cdot}E$ VALUES DERIVED FROM α/β PHASE BOUNDARIES

	Δn	S	$\Delta^{\cdot}E$
Zr-Ag	-1	49	-.075
Zr-Cu	-1	313	-.134
Zr-Ti	0	71	-.033
Zr-In	+1	1	+.049
Zr-Al	+1	121	+.022
Zr-Sn	+2	7	+.060
Zr-Pb	+2	46	+.035
Zr-Sb	+3	42	+.073

	Δn	S	$\Delta^{\cdot}E$
Ti-Ag	-1	2	-.019
Ti-Au	-1	2	-.050
Ti-Cu	-1	104	-.084
Ti-Zr	0	85	-.024
Ti-Al	+1	8	+.039
Ti-Ge	+2	193	+.014
Ti-Sn	+2	144	-.032
Ti-Si	+2	303	-.065
Ti-Pb	+2	272	-.067

The entropy values used above for the α/β transitions in pure zirconium and titanium were 3.491×10^{-5} e.v./atom-deg[20] and 3.541×10^{-5} e.v./atom-deg[18], respectively.

$K_2 = -3.2 \times 10^{-4}$ e.v./atom and for the titanium alloys $K_1 = 0.033$ e.v./electron and $K_2 = -4.4 \times 10^{-4}$ e.v./atom. The similarity of these numbers for the zirconium and titanium systems was encouraging since both zirconium and titanium would be expected to behave similarily and both sets of data were combined to obtain the average values .030 (K_1) and -3.9×10^{-4} (K_2).

CALCULATION OF PHASE BOUNDARIES FROM AVERAGE PARAMETERS

The agreement of a particular zirconium or titanium system with these two average constants is by no means perfect, and other complicating factors are undoubtedly present which have not been discussed. However, in order to illustrate the degree of agreement, under the earlier approximations that $\ddot{E}_{o\alpha}\ddot{E}_{o\beta}\ddot{C}_{\alpha}\ddot{C}_{\beta}$ and $\Delta^{\cdot}C$ all vanish, equation (1) has been used to recalculate the α/β phase boundaries for some typical systems. This calculation is also of interest in order to see how well the nature of the derived boundaries and the distance between them correspond to experiment.

These results are illustrated in Fig. 18 (ORNL-LR-DWG 18984). The agreement is reasonably satisfactory for the systems Zr-Cu and Zr-Sn and to a lesser extent for the systems Ti-Ag, Ti-Al, Zr-In, and Zr-Pb[22]. The systems, Ti-Cu, Ti-Au, and Zr-Ag, all show greater alpha solid solubility by calculation than in the experiment. This may be related as discussed earlier, to the impurities in the iodide crystal bar. In at least two systems Zr-Ag and Zr-In the reduction in impurities has lead to better agreement with the calculation as the experimental work progressed.

The effects of transition element solutes have been omitted in the previous discussion because their valency as solutes is likely to be variable in different alloys. However, since important impurity effects arise from these elements the boundaries have been calculated for the case of Zr-Fe under the assumption that iron acts with a valency of zero in this system. Unusually low solid solubility of iron in alpha zirconium in this way appears to be consistent with this valency and a large size factor.

The system Zr-Ti is also of interest since no valency change would be expected in this system, and here the variation of the α/β boundaries appears to be quite well reproduced by the relative stain energy term alone.

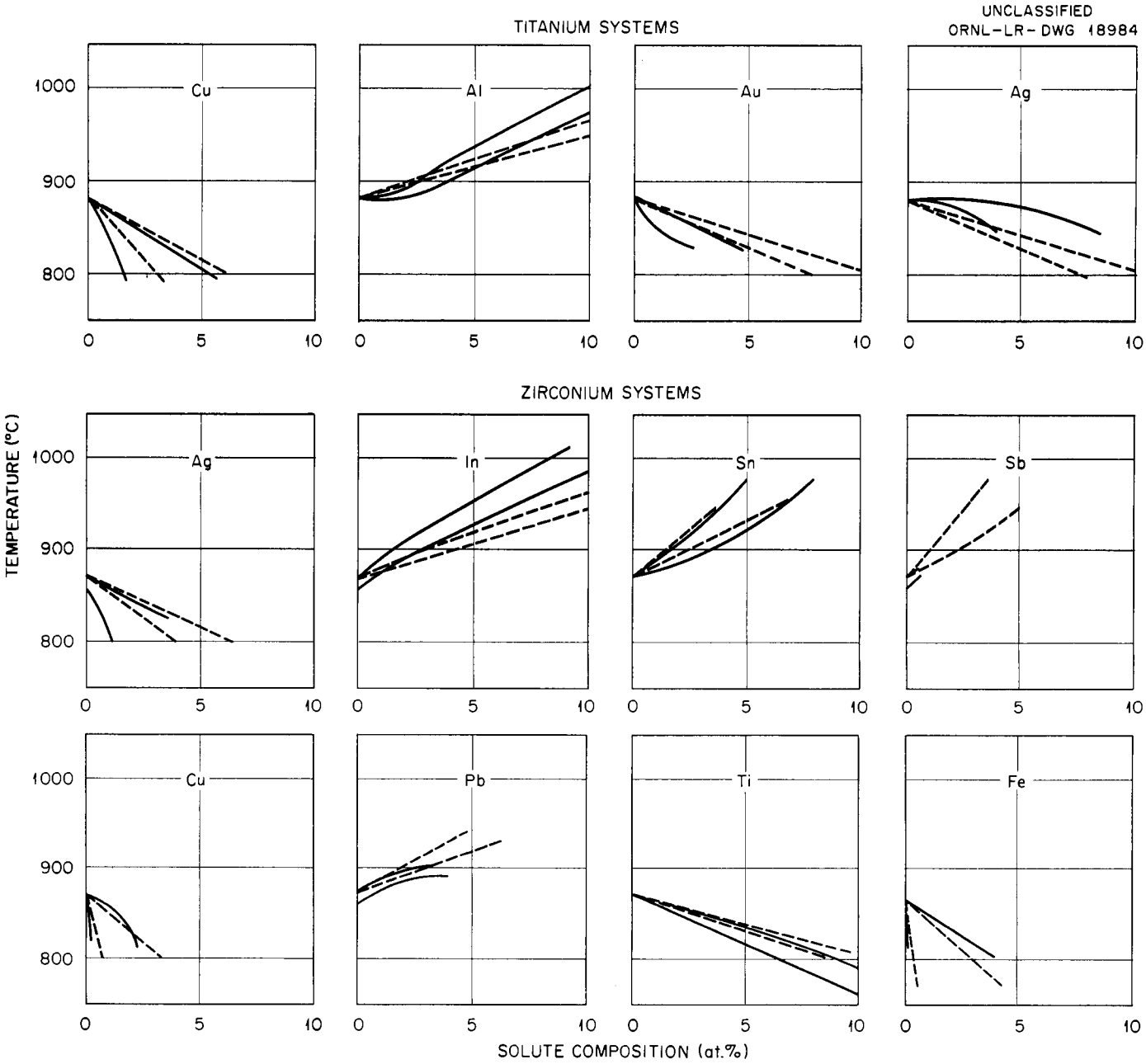

Fig. 18. Comparison of Experimental α/β Boundaries (solid lines) with Calculated Results (dotted lines)

DISCUSSION OF THE ENERGY PARAMETERS AND THE DIVALENCY OF GROUP IVA ELEMENTS

In the above, the square of the size factor was used so that the constant obtained would correspond to a rough estimate of the relative strain energy by means of the formula, $W = 8\pi\, r_o\, (G)\, (r-r_o)^2$, where W is the strain energy in an isotropic elastic medium due to the insertion of a rigid sphere of radius r in a single spherical cavity of radius r_o[23]. If percentage differences are used as in the graphs this formula becomes

$$W = 8\pi r_o^3\, G\, 10^{-4}\, \left(100\, \frac{r - r_o}{r_o}\right)^2$$

In the present case the approximation is made that the solute atoms act as if they were rigid spheres and the rigidity modulus in both forms of zirconium at the transition temperature T_c is estimated from measurements of Youngs Modulus by Koster[24]. The result obtained $\Delta^{\cdot}E = -1.6 \times 10^{-4}\, \left(100\, \frac{r - r_o}{r_o}\right)^2$ e.v./atom is smaller than that derived from the experimental results but it is of the correct order of magnitude.

The other constant K_1 obtained from this fitting of the phase boundaries is equal to $\Delta^n E_o$ or $\frac{\partial}{\partial n}(E_{o\beta} - E_{o\alpha})$. This can be seen by writing $\Delta^{\cdot}E_o = K_1\, \Delta n$ for a case of zero size factor and transforming the compositional variable to electron concentration. More experimental work is required to assign a definite interpretation to this parameter but for the present its meaning might be understood by assuming that the only energy term which changes differently in the two phases during alloying is the energy of the valency electrons $\int_o^n \epsilon dn$ where ϵ represents the electron energy. If the valency band is assumed rigid in alloying for small changes in $(n - n^o)$, then the energy of the alloy phase can be expanded as a Taylor's series.

$$E_{o\beta} = \int_o^{n^o} \epsilon_\beta\, dn + \epsilon^o_\beta\, (n - n^o) + \frac{(n - n^o)^2}{2N(\epsilon)^o_\beta} + \ldots$$

Thus to a first approximation, neglecting the second and higher powered terms, $\frac{\partial}{\partial n}(E_{o\beta}) = \epsilon^{o}_{\beta}$, $\frac{\partial}{\partial n}(E_{o\alpha}) = \epsilon^{o}_{\alpha}$, and $\Delta^{n}E = \epsilon^{o}_{\beta} - \epsilon^{o}_{\alpha}$. A difference of 0.03 e.v./atom in the Fermi surfaces of the two phases, the lower temperature allotrope having the lower Fermi surface, would thus be sufficient to account for the numeral value of this constant.

The most interesting result obtained from the α/β phase boundaries is the valency of two for zirconium and titanium. Theoretical calculations of the energy states in titanium and zirconium have not been made in sufficient detail to permit an explanation to be made. However, in many discussions of transition elements the electrons are regarded as occupying two separate distributions, one an s-type band, and the other a d-type band. One characteristic of the d-type band is that it is more tightly bound to the atom and if in the present case of alloying zirconium or titanium the d electron band is assumed not to extend into the atomic cells of the solute atoms, then it is easily shown that successive removal of zirconium and titanium atoms during alloying could remove four electrons and one "d" state, resulting in an effective valency of two as far as movements of the Fermi surface are concerned.

LIST OF TABLES

Table		Page
I	Analyses of Iodide Zirconium Used in the Phase Diagram Studies	3
II	Typical Annealing Times in Phase Diagram Investigations	5
III	Minor Impurity Analyses of Alloys	7
IV	$\Delta^{\cdot}E$ Values Derived from α/β Phase Boundaries	42

LIST OF ILLUSTRATIONS

Figure			Page
1	ORNL-LR-DWG 16110	Silver-Zirconium Equilibrium Diagram According to Kemper	10
2	ORNL-LR-DWG 15394	Preliminary Investigation of the Eutectoid Region of the Silver-Zirconium System	11
3	ORNL-LR-DWG 18989	Final Investigation of the Eutectoid Region of the Silver-Zirconium System	13
4	Y-16703, -16696, -16782, -17100	Three-Phase Microstructures of Alloy Containing 2.1 At. Per Cent Silver	14
5	ORNL-LR-DWG 16109	Thermal Arrests in Silver-Zirconium Alloys in the Region 0-10 At. Per Cent Silver	16
6	ORNL-LR-DWG 18988	The Silver-Zirconium Phase Diagram in the Region 0-36 At. Per Cent Silver	18
7	ORNL-LR-DWG 16329	Preliminary Investigation of the Indium-Zirconium Phase Diagram in the Region 0-28 At. Per Cent Indium	22
8	Y-9798, -10814 -10993	Microstructures of In-Zr Alloys	23
9	ORNL-LR-DWG 18987	Final Investigation of the Indium-Zirconium Phase Diagram in the Region 0-13 At. Per Cent Indium	25
10	ORNL-LR-DWG 8133	Effect of Impurities on the Variation of the Volume Proportion of Alpha and Beta Phases in the ($\alpha + \beta$) Region at 900°C	26
11	ORNL-LR-DWG 18983	Preliminary Investigation of the Antimony-Zirconium Phase Diagram in the Region 0-6 At. Per Cent Antimony	28
12	ORNL-LR-DWG 16274	Peritectoid Region of the Antimony-Zirconium Phase Diagram, According to the Preliminary Investigation	29

LIST OF ILLUSTRATIONS (Con't)

Figure			Page
13	ORNL-LR-DWG 16272	Final Investigation of the Peritectoid Region of the Antimony-Zirconium System	31
14	ORNL-LR-DWG 18986	Position of the Phase Boundaries Between the Allotropic Forms of Zirconium, Titanium, and Cobalt with Solutes of Different Valency	33
15	ORNL-LR-DWG 16106	The Variation of the Temperature of the α/β Phase Boundaries in Titanium Systems with Electron Concentration	34
16	ORNL-LR-DWG 16107	The Variation of the Temperature of the α/β Phase Boundaries in Titanium Systems with Electron Concentration	36
17	ORNL-LR-DWG 18985	Relative Energy Change with Alloying of the Alpha and Beta Phases Calculated from the $\alpha/(\alpha + \beta)$ and $\beta/(\alpha + \beta)$ Phase Boundaries of the Ag-Zr and In-Zr Systems	40
18	ORNL-LR-DWG 18984	Comparison of Experimental α/β Boundaries (solid lines) with Calculated Results (dotted lines)	45

REFERENCES

1. W. Hume-Rothery, G. W. Mabbott and K. M. Channel-Evans, Phil. Trans. Roy. Soc. 1934, (A), 233, 1.
2. W. Hume-Rothery and G. V. Raynor, Jour. Inst. Metals, 1937, 61, 208.
3. E. Raub and M. Engel, Z. Metallkunde, 1948, 39, 172.
4. C. T. Anderson, E. T. Hayes, A. H. Roberson and W. J. Kroll, Report of Investigation 4658, U. S. Bureau of Mines, 1950.
5. R. S. Kemper, Jr., "The Zirconium-Silver System", Oregon State College Thesis, 1952.
6. N. Karlsson, Acta Chem. Scand., 1952, 6, 1424.
7. E. T. Hayes, A. H. Roberson, and W. L. O'Brien, Trans. Amer. Soc. Met., 1951, 43, 888.
8. R. F. Russi, Jr., and H. A. Wilhelm, U. S. Atomic Energy Commission Publ., 1951, (AECD 3610), (ISC-204).
9. B. Lustman and F. Kerze, Jr., The Metallurgy of Zirconium, New York, 1955.
10. The curve for Cd-Zr is based on unpublished data by D. S. Easton and J. O. Betterton, Jr.
11. F. Wever, Archiv Eisenhütten Wesen, 1928-9, 2, 739.
12. W. Koster, Z. Metallkunde, 1952, 43, 297.
13. A. D. McQuillan and M. K. McQuillan, Titanium, London, 1956.
14. G. V. Raynor, Proc. Roy. Soc., 1942, (A), 180, 107.
15. E. A. Owen, J. Inst. Metals, 1947, 73, 478.
16. H. J. Axon, and W. Hume-Rothery, Proc. Roy. Soc., 1948, (A), 193, 1.
17. H. Jones, Proc. Phys. Soc., 1937, 49, 243.
18. G. Skinner, H. L. Johnston, and C. Beckett, Titanium and its Compounds, 1954 (H. L. Johnston Enterprises, Columbus, Ohio).
19. The Reactor Handbook, Vol. 3, Sec. 1, United States Atomic Energy Commission publication, AECD-3647, 1955, p. 464.

REFERENCES (Con't)

20. J. P. Coughlin and E. G. King, Jour. Amer. Chem. Soc., 1950, 72, 2262.

21. Metals Handbook Supplement, Amer. Soc. for Met., 1954, p. 87.

22. The experimental curve for Zr-Pb in Fig. 19 is based on unpublished data by G. D. Kneip, Jr. and J. O. Betterton, Jr.

23. M. A. Jaswon, W. G. Henry, and G. V. Raynor, Proc. Phy. Soc., 1951, (B), 64, 182.

24. W. Koster, Z. Metallkunde, 1948, 39, 1.